PROCEEDINGS B

rspb.royalsocietypublishing.org

Research

Cite this article: Rooker K, Gavrilets S. 2018 On the evolution of visual female sexual signalling. *Proc. R. Soc. B* **285**: 20172875. http://dx.doi.org/10.1098/rspb.2017.2875

Received: 28 December 2017
Accepted: 30 April 2018

Subject Category:
Evolution

Subject Areas:
evolution, theoretical biology, behaviour

Keywords:
ovulation, female mating competition, male mate choice, infanticide, modelling

Author for correspondence:
Sergey Gavrilets
e-mail: gavrila@utk.edu

Electronic supplementary material is available online at https://dx.doi.org/10.6084/m9.figshare.c.4096418.

THE ROYAL SOCIETY PUBLISHING

On the evolution of visual female sexual signalling

Kelly Rooker[1] and Sergey Gavrilets[1,2,3]

[1]Department of Mathematics, [2]Department of Ecology and Evolutionary Biology, and [3]National Institute for Mathematical and Biological Synthesis, University of Tennessee, Knoxville, TN 37996, USA

KR, 0000-0002-2489-0189

A long-standing evolutionary puzzle surrounds female sexual signals visible around the time of ovulation. Even among just primates, why do some species have substantial sexual swellings and/or bright colorations visible around females' genital regions, while other species are like humans, with no signs of ovulation visible? What is the evolutionary purpose behind not just these signs, but also this great variation seen among species? Here, we examine the evolutionary trade-offs associated with visual ovulation signalling using agent-based modelling. Our model predicts how various factors, including male genetic heterogeneity and reproductive inequality, female physiological costs, group size, and the weighting of genetic versus non-genetic benefits coming from males, each influence the strength of ovulation signalling. Our model also predicts that increasing the impacts of infanticide will increase ovulation signalling. We use comparative primate data to show that, as predicted by our model, larger group size and higher risk of infanticide each correlate with having stronger visual ovulation signs. Overall, our work resolves some old controversies and sheds new light on the evolution of visual female sexual signalling.

1. Introduction

Two general components of sexual selection are mate competition and mate choice [1,2]. Traditionally, mate competition has been associated with *male–male* competition for access to females, while mate choice with *female* choice (for example, the bright colours, exaggerated plumage and mating displays seen among males in many different species of birds to attract female mates) [2–6]. However, there are now multiple examples of *female–female* competition (e.g. competition among female chimpanzees for space and food [7]) and *male* mate choice (e.g. males preferentially mating with females of a specific age and mating call); see Clutton-Brock [8] for a review and Servedio & Lande [9] for modelling work.

A striking example where female–female competition and male mate choice may be occurring is visual female sexual signalling in primates [10,11]. Visual signals around a female's time of ovulation are widespread across primate phylogeny [12], and such signs are thought to have evolved independently at least five times among the catarrhine primates (i.e. Old World monkeys and apes) [13]. Although much varied between species, these signals primarily occur via changes in the size, swelling, shape and/or colour of the female's perineal skin [13,14]; see figure 1 for an example.

Visual ovulation signals clearly have significant costs [15]. Physiologically, swellings resulting from increased water retention, increased body weight, as well as diverting fluids away from potentially more important bodily functions (especially in dry/drought conditions) [16]. Higher body weight (making mobility more challenging), noticeable swellings and/or genital colorations can increase a female's risk of predation. Sexual swellings expose the female's perineal skin to parasites, as well as to cuts and scratches [12]. Visual ovulation signs can also result in social costs, for example, if increased within-group male competition hurts the group's success in between-group conflicts, leading to a reduction in the

Figure 1. Olive baboons in Gombe National Park, Tanzania (photograph by Dr Michael Wilson). Adult female with sexual swelling (left) being groomed by an adult male (right).

group's territory and/or food resources, and/or increased infant deaths as a result of the between-group encounters [17–19].

Given all these costs, the evolution of visual female sexual signalling was long viewed as a puzzle. In addition, its lack thereof in humans when compared with chimpanzees was also long-debated [20–23]. Various potential benefits of having visual ovulation signs have been proposed, each emphasizing different selective forces. For example, when female–female indirect competition is at play, females can signal that they are fertile [24] or of high quality [25] to simplify fertilization or to obtain good genes for their offspring. When mating opportunities are limited at least for some males, females can also signal to obtain direct benefits such as provisioning or protection by males of ovulating females (defence against injury, predation and harassment) [12]. Other benefits may instead help females' offspring; for example, having visual ovulation signals could help females increase males' perceived probabilities of paternity [12,26] which could lead to offspring protection or paternal care [27,28]. This would be important in the presence of infanticide (see below). Many of the above selective forces and benefits could be working in tandem, depending on the exact combination of sexual selection dynamics occurring.

Earlier discussions of the evolution of visual ovulation signs were often framed in terms of two female mating tactics: 'paternity concentration' and 'paternity confusion'. The former emphasizes female–female competition for better mates in order to receive benefits, whether genetic or non-genetic, to their offspring or themselves [17]. The latter emphasizes matings with multiple males. Having more than one mating partner can be helpful in the presence of genetic (or gametic, immunological, etc.) incompatibilities, post-copulatory sperm competition (cryptic female choice), male investment in offspring, etc. [6,15,29–31]. Doing so allows a female to make more than one male think he may be the father of her offspring (i.e. confuse paternity), which can be beneficial, for example, in reducing the risk of infanticide for the female's offspring [15,32].

Infanticide, the killing of a female's offspring prior to weaning, is extremely detrimental to a female's fitness [24,32–35]. However, committing an act of infanticide may benefit any male who is not the father of that particular offspring, and hence infanticide is often seen when a new male takes over a group [36]. Many primate species have prolonged lactational amenorrhoea [37], resulting in a male killing a female's offspring bringing that female back to fertility sooner by prematurely ending her lactation [38,39]. The infanticidal male can then subsequently mate with this female, meaning his offspring will be able to be born sooner than would otherwise be possible had he never committed infanticide [31]. Although infanticidal events are typically rare, they have been documented in many primate species [32] and can constitute a substantial proportion of infant mortality in some primate species [6].

Over time, neither paternity concentration nor paternity confusion obtained a consensus on being the more likely benefit [12]. Two new evolutionary hypotheses were then proposed, attempting to take into account more selective forces and help reconcile the benefits of paternity concentration with the benefits of paternity confusion. The first, the reliable indicator hypothesis, claims that female–female competition drives visual sexual signals to be reliable indicators for males of each female's quality during that competition [25]. Females are actively seeking high-quality males and, were it beneficial, high-quality females would also be able to attract more than one quality male [25].

The second, the graded signal hypothesis, explicitly recognizes the fact that visual sexual signals serve as 'graded signals' for females, i.e. such signals are probabilistic, increasing and decreasing in strength gradually, with ovulation often happening around the time of a female's peak signal. In doing so, a female is able to attract male(s) with good genes around the peak of her signal (i.e. when she is probably most fertile), while still attracting other, lesser quality male(s) during other parts of her cycle (when she still has some sexual signal, just not at its peak, and is probably less fertile) [12].

Although often presented as opposites, both the reliable indicator and graded signal hypotheses invoke female competition for high-quality males and both implicitly assume that females are competing for high-ranking males because those males have superior genetic quality. However, in many cercopithecine primates, male rank is a function of age, rather than of good genes [13]. Note the reliable indicator hypothesis is quite vague about what fitness benefits females might be obtaining through competition. One of the advantages of our approach—as shown later—is explicit consideration of both genetic and non-genetic components.

Substantial field and laboratory work (e.g. [40–48]), as well as phylogenetic studies (e.g. [12,49,50]), have all been done in order to help understand visual ovulation signalling in an evolutionary context. As a result of all this work, the graded signal hypothesis is now largely recognized as being the hypothesis to explain the evolution of visual female sexual signalling, while the reliable indicator hypothesis was unable to find support empirically, and has fallen out of favour [12,28,42,44,47].

Many questions, however, still remain. For example, as related to infanticide, is it more likely for infanticide to serve as selection pressure for the evolution of concealed ovulation or of visual sexual signals? It has long been thought that infanticide could be a main selection pressure for *concealed* ovulation to evolve (e.g. see [29,32]). A female with concealed ovulation would have the vast majority of her cycle to confuse paternity (lowering her offspring's risk of infanticide) and would not have to suffer any of the physiological costs of having visual ovulation signs [32].

Completely opposite these beliefs is, as discussed earlier, the idea that females who signal prominently are better able to attract multiple males as mating partners, which (for example) is beneficial in reducing the risk of infanticide occurring to that female's offspring by confusing paternity [15]. Supporting this hypothesis are the facts that females with peak signals often mate with multiple males [51] and that such signals are not perfectly honest; ovulation does not always occur exactly at the time of a female's peak signal [12,48]. Indeed, like this example of infanticide above, many of the proposed benefits of having visual ovulation signs have also instead been proposed as *costs* to females. As Austin Burt says, 'Ironically, there is considerable overlap between the hypothesized benefits of sexual signals and those of concealed ovulation.' [26, p. 4].

Informative experiments relating to this phenomenon are by nature rather challenging to conduct, and many ideas historically have just been presented as verbal arguments which can often be easily challenged. Despite still-unanswered questions on the role and evolution of visual female sexual signalling, even just within the context of the graded signal hypothesis, there has been relatively little theoretical work done in understanding the evolutionary trade-offs behind these signs persisting in so many different species (but see [25,52,53]). In fact, two different reviews of visual ovulation signalling appealed specifically for '[More] theoretical approaches [to] be undertaken' [12, p. 241] and 'More rigorous modelling, using mathematical tools and simulation approaches, [being] needed' [11, p. 83].

With only two modelling attempts published after these calls (discussed later), the area is ripe for improved theoretical work. Hence, it is our aim here to use mathematical modelling to help explore the evolutionary trade-offs associated with visual female sexual signalling. Note that it is not our goal here to test specific verbal arguments against one another, for example, the reliable indicator versus graded signal hypotheses. Rather, allowing for multiple evolutionary forces (including different types of selection) known to act in the populations of our models, we are interested in determining under what conditions will ovulation signalling increase and/or decrease in a multi-male, multi-female population, assuming such signals to be graded. Compared to earlier, limited modelling efforts [25,52,53], our models explore a much wider range of evolutionary factors under more biologically realistic assumptions. In particular, we explicitly allow for infanticide, consider genetic and non-genetic benefits to females, and assume that males estimate their female mates' fertilities, rather than know them exactly.

2. Material and methods

First, we use mathematical modelling, and then we conduct statistical analyses of empirical data in order to test two of our model's predictions.

(a) Model

We consider a population of individuals living in a large number of groups each with N males and N females. Generations are discrete and non-overlapping. Next, we outline major modelling components; see appendix A for full model details.

Females. We explicitly account for the female cycle, which we split into D discrete units of time. While such units could be hours, minutes, etc., we choose to call such units 'days' (for example, with 29 days in one female cycle). Each female is fertile for C days of this cycle; the distribution of probabilities of fertilization across the cycle has the same shape for all females but is randomly centred (meaning cycle synchrony may only occur probabilistically). Females differ genetically in visual ovulation signs present. We assume both ovulation and maximum visual ovulation signs to happen directly in the middle of each female's C fertile days so that there exists at least some reliability of the ovulation signal. We treat visual ovulation signs, $x(d)$ for each day d of the cycle, as overlapping curves (see fig. 11.1 of [13] for comparison). Each female is characterized by two genetically controlled, evolvable traits. Magnitude m is the maximum amount of ovulation signs a female has visible during her cycle; m is a non-negative, continuous number. Length ℓ is the number of days a female has *some* amount of ovulation signs visible; ℓ is a non-negative, integer number. Ovulation signs are costly; these costs are scaled by parameter c. For an example of what these ovulation signs $x(d)$ could look like across a cycle for four females with varying values of m and ℓ see figure 2.

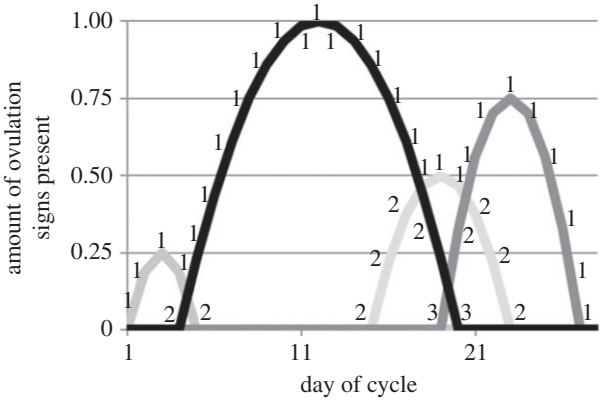

Figure 2. Example ovulation signs for females with different trait values over one 29 day cycle. Different colours represent four different female cycles. Numbers beside each curve represent the rank of the male's genetic component (GC) who is most probably to mate with the female on that particular day of her cycle (assuming no reproductive stochasticity).

Males. We assume males to differ in 'quality', i.e. any benefit from the male to a female and/or her offspring. Variation in male quality is scaled by parameter b, which also characterizes female benefits. Such quality is explicitly split into a genetic component y_g (GC) and a non-genetic component y_{ng} (NGC). GC is owing to the male's genes being passed to the female's offspring, while NGC is any non-genetic benefit to the female from mating with that male. For example, NGC could be protection provided to the female herself or increased food, provisioning, access to resources, etc. (as reviewed in detail in [6]). We allow for y_g to correlate with male's rank (and hence his success in reproductive competition). (Note however that, as we show below, females can still evolve to signal ovulation even with no genetic benefits included in the model.) We also allow for correlation ρ between y_g and y_{ng}. For example, $\rho < 0$ corresponds to the case when powerful males are less interested in providing any protection/provisioning to females. $\rho > 0$ instead corresponds to the case when being a more powerful male implies being better at protecting/provisioning females. We do not consider evolution in males, assuming instead that male traits are at a (stochastic) evolutionary equilibrium.

Mating pairs. For every unit of time in the cycle, all males and all females in each group enter the competition for mates. For computational simplicity, we assume each individual to mate exactly once on every unit of time (e.g. day). Males of higher rank (and GC) are more likely to mate with females with stronger ovulation signs visible (higher $x(d)$), i.e. when the female is most likely to be most fertile. Males of lower rank (and GC) mate with

females who have fewer ovulation signs visible, i.e. when the female is less likely to be most fertile. For empirical support of this assumption in primates, see [41,43,45]. However, this assumption can be relaxed via reproductive stochasticity. The degree of reproductive stochasticity in males and females is controlled by parameters $\epsilon_m \geq 0$ and $\epsilon_f \geq 0$, respectively. With $\epsilon_m = \epsilon_f = 0$, mating pairs are formed deterministically so that the highest GC male mates with the female with the most ovulation signs visible, and so on (figure 2); this is the case of perfect assortment in mating. Increasing ϵ_m increases stochasticity in the outcome of male competition for mating success, and thus reduces male reproductive inequality. Increasing ϵ_f reflects a decrease in the reliability of the ovulation signal as well as a lack of opportunity or interest for fertile females to mate with a higher GC male (e.g. as shown empirically in Amboseli baboons [47]). With large ϵ_m, ϵ_f, mating becomes random.

Reproduction. For any female's potential offspring, every male in the group has an associated probability of paternity, ranging anywhere from zero to one. This quantity is determined by both the number of times that particular male mates with the female during her cycle, as well as her probability of fertilization on the days of each mating event. Assuming additivity of cost and benefit effects for simplicity, we specify female fitness (fertility) as:

$$\begin{aligned}\text{female fitness} = {} & \text{baseline female fitness} \\ & + (1-\eta) * (\text{genetic quality of the father}) \\ & + \eta * (\text{average non-genetic quality over all mates}) \\ & \pm \text{effect of infanticide from all males} \\ & - \text{cost of having visible ovulation signs.}\end{aligned}$$

Here, $0 \leq \eta \leq 1$ specifies the relative weight of the NGC; with $\eta = 0.5$, male-provided genetic and non-genetic benefits are equally important for females. Fitness is each female's relative reproductive success, i.e. the expected number of offspring surviving to the age of reproduction, normalized to keep the total population size in each generation constant. Offspring production is followed by dispersal.

Infanticide. Modelling infanticide is adapted from [24]. Any male is able to help or harm (note 'harm' here could simply mean not helping) an offspring prior to the infant being weaned, although some males (e.g. those of higher quality, size or strength) are able to do so more effectively. Our model does not distinguish between the threat of infanticide via an outsider male or a previously subordinate male. Infanticide's effects on offspring viability are scaled by parameters α (maximum benefit of protection from infanticide) and β (relative maximum cost of infanticide). An additional parameter $0 \leq \kappa \leq 1$ determines the extent to which males take visible female ovulation signs into account when estimating their paternity in determining what actions to take regarding infanticide. $\kappa = 0$ means males estimate their probability of paternity solely by the number of matings with an offspring's mother, while $\kappa = 1$ means males instead estimate paternity exclusively on the basis of the female's visible ovulation signs during their time of mating.

Our goal here is to understand how visual female ovulation signs evolve over time. Appendix A provides further details, explicit fitness functions and full definitions of equations and parameters.

(b) Testing hypotheses against data

We were able to aggregate enough data from extant primate species living in multi-male, multi-female groups to test two of our model's predictions. All data are available in the electronic supplementary material. Note that all of our data sources are data collections from primatologists whose methods and results have already been published elsewhere; we did not do any data collection ourselves. Also note we restricted these analyses to those primate species with a polygynandrous mating system because our model explicitly considers primate individuals living in multi-male, multi-female groups and mating system is already a known correlate of visual ovulation signs in primates [49,50].

Wherever available, we aggregate data per species for: (i) visible ovulation signs, (ii) group size and (iii) risk of infanticide. Ovulation signs data were available from [15,49,50,54]. We follow [50] in grouping 'absent' and 'slight' ovulation signs visible (e.g. from the ternary classification as found in [49]) together into the one category of 'absent'. This is owing to both the fact that the category 'slight' is vague (e.g. does a species whose females have no sexual swellings, but just a barely visible reddening of the perineum count as 'absent' or 'slight'?) and also that it has yet to be established that males use 'slight' swellings as any kind of signal [50]. Average group size was aggregated from [55–58] for each species for which data were available. For infanticide risk, we used Opie *et al.*'s data on lactation and gestation length [59]. The average ratio of L/G: = lactation length/gestation length is a known correlate of infanticide risk, with species with higher L/G having higher risks of infanticide [37].

For the first analysis, we compare visible ovulation signs with group size. Doing so gives 65 species with both a classification of having 'present' or 'absent' visual ovulation signs and the species' average group size. We use this to compare the average group sizes for species with absent versus present visual ovulation signs. To test for significance, we control for phylogeny using a simulation-based phylogenetic ANOVA test [60,61] with a recent primate phylogeny [62].

For the second analysis, we compare visible ovulation signs with risk of infanticide. Doing so gives 48 species with both a classification of 'present' or 'absent' visual ovulation signs, and a value of L/G. We use this to compare the distributions of L/G for species with absent versus present visual ovulation signs. To include phylogeny, we fit a likelihood-based model of continuous trait evolution (see [63] for specific details of the method), again using the primate phylogeny from Fabre *et al.* [62]. We fit both Brownian motion and Ornstein–Uhlenbeck models using the *R* package *OUwie* [63]. In particular, we compare Ornstein–Uhlenbeck models with one versus multiple optima for L/G. In the case of only one single optimum, the trait is assumed to evolve non-neutrally, but that all species (regardless of present versus absent visible ovulation signs) are pulled towards that one single optimal value of L/G. With multiple optima (one for species with present visible ovulation signs and the other for species with absent visible ovulation signs), species with present versus absent visible ovulation signs have different average values of L/G. In all cases, the Akaike information criterion (AIC) was calculated from the likelihood to compare the fit of the models, which each made the different evolutionary assumptions. See the electronic supplementary material for a further description of this method, additional results and discussion on method choice.

3. Results

Model. Agent-based simulations of our model show that the average values of the ovulation signs magnitude trait (m) and the ovulation signs length trait (ℓ) converge to the unique equilibria m^*, ℓ^*. Note in most simulations, $\ell^* \leq 7$, because we set the time of fertility C to 7 days. A more comprehensive discussion of our simulations and the effects of parameters can be found in the electronic supplementary material.

Figure 3*a* summarizes the effects without infanticide of the benefit b, cost c, and group size N on the equilibrium values m^* and ℓ^*. As expected, increasing benefits b and decreasing costs c each result in increased m^*, ℓ^*. Our simulations also show that increasing group size N results in increased m^*. This is because increasing the number of females in each group intensifies female–female competition

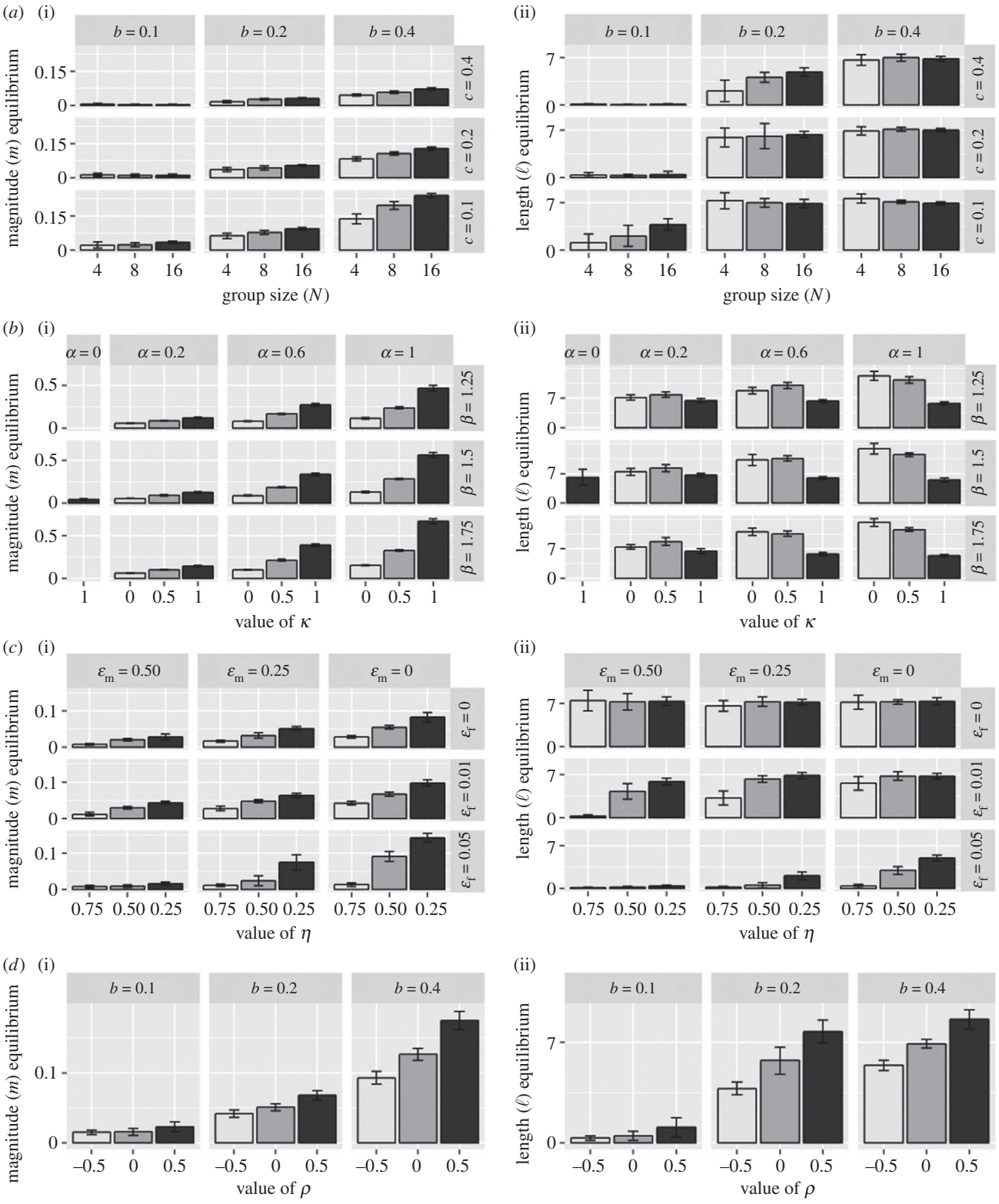

Figure 3. Effects of parameters on the average equilibria values of ovulation signs magnitude (m^*, i) and ovulation signs length (ℓ^*, ii). (*a*) The effects of variation in male quality (*b*), costs of having visual ovulation signs (*c*) and group size (*N*). (*b*) Effects relating to infanticide (α, β, κ). $\alpha = 0$ represents the case with no infanticide present (and hence when β, κ are irrelevant). (*c*) The effects of reproductive stochasticity in males (ϵ_m) and females (ϵ_f) and the relative weighting of NGC (η). (*d*) The effects of variation in male quality (*b*) and correlation between a male's GC and NGC (ρ). Equilibria are obtained by averaging 16 initial condition runs (with standard deviation indicated by error bars). Other parameters: (*a*) $\epsilon_m = 0.25$, $\epsilon_f = 0.01$, $\alpha = 0$, $\gamma = 1$, $\eta = 0.5$, $\rho = 0$; (*b*) $N = 8$, $b = 0.2$, $c = 0.2$, $\epsilon_m = 0.25$, $\epsilon_f = 0.01$, $\gamma = 1$, $\tau = 2$, $\omega = 1$, $\eta = 0.5$, $\rho = 0$; (*c*) $N = 8$, $b = 0.2$, $c = 0.2$, $\alpha = 0$, $\gamma = 1$, $\rho = 0$; (*d*) $N = 16$, $c = 0.1$, $\eta = 0.75$, $\epsilon_m = 0.25$, $\epsilon_f = 0.01$, $\alpha = 1$, $\gamma = 1$.

for high GC males [6], which incentivizes having more visual ovulation signs present with which to attract such males.

Figure 3*b* instead summarizes the effects of parameters relating to infanticide (α, β, κ) on the equilibrium values of m^* and ℓ^*. Increasing the effects of infanticide α and β, and the relative weight of female ovulation signs in males' paternity estimations κ each results in increased values of m^*. Intuitively, as these effects relating to infanticide increase, it becomes in females' best interests to mate with high GC males (i.e. males more likely to have their actions be effective within their group,

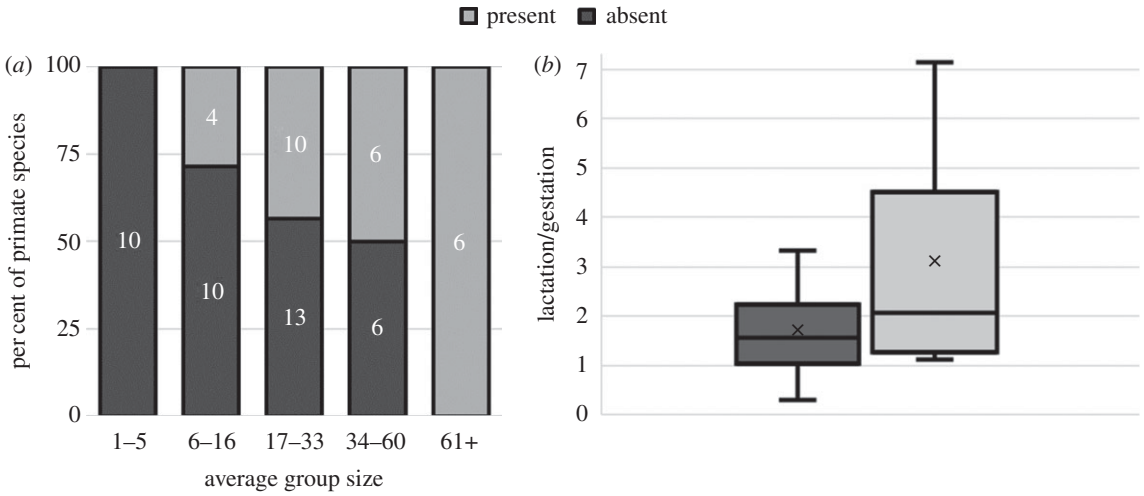

Figure 4. (*a*) Comparing primate species' average group size by females having 'present' or 'absent' visual ovulation signs. After controlling for phylogeny, species with higher group sizes are more likely to have visual ovulation signs, and species with concealed ovulation smaller group sizes (using phyloANOVA: $F = 12.868$, $p = 0.002$). Numbers inside the bars indicate the numbers of species contained in each category. (*b*) Box plots depicting the distributions of L/G for species with each 'absent' (33 species) and 'present' (15 species) ovulation signs. Including phylogeny, the model with 'absent' and 'present' having distinct means has a 62% relative probability. Each box plot depicts the minimum, maximum, median, and quartile values, while the black x's mark the means.

whether owing to strength, rank, etc. and hence be better able to help protect an infant). Increased matings then give these males increased likelihoods of being the father of any subsequent offspring that female produces, which increases the likelihood of the male attempting to protect the offspring against any possible infanticide being committed. Having strong visual ovulation signs facilitates such matings with high GC males.

Figure 3*c* summarizes the effects without infanticide of the relative weight of male-provided non-genetic benefits η and the two reproductive stochasticity parameters, ϵ_m and ϵ_f. Decreasing η increases the value of the 'prize' to a female for winning the female–female competition for good genes, thus incentivizing increased visible ovulation signs with which to attract high GC males. Note these effects of η are in line with empirical work, for example; see [6,28]. In general, the more reproductive stochasticity present, the smaller the benefit to a female of having visible ovulation signs, meaning the smaller her ovulation signal. Increasing male reproductive stochasticity (meaning decreasing the amount of reproductive inequality among males) decreases the female ovulation traits m^*, ℓ^*. With more male reproductive stochasticity, strongly signalling females are less likely to get mates with high GC males, simply by chance, leading to females investing less energy in such signalling. With high reproductive stochasticity among males, high reproductive stochasticity among females effectively takes away any benefit to females of having visible ovulation signs (i.e. the benefit from winning the female-female competition for high GC males), leaving such signs only as a cost and why both m^*, ℓ^* sharply decrease in the case of large male *and* female reproductive stochasticity.

In many situations, parameter ρ (the correlation between males' GC and NGC) does not have much of an effect (see the electronic supplementary material). However, when ρ *does* have an effect, increasing ρ will result in increased m^*, ℓ^*. Such an effect will appear with larger benefit b, larger relative weight of non-genetic benefits η, and smaller reproductive stochasticity in females ϵ_f. Figure 3*d* illustrates one such scenario. In general, visible ovulation signs will increase when females benefit from attracting high GC males. With larger ρ, high GC males are increasingly also high in NGC, thus doubling the benefit an attracting female would receive from them. Indeed, as figure 3*d* illustrates, ρ intuitively has larger effects with higher b, meaning when such quality coming from high GC males is the greatest. In addition, ρ will have larger effects with larger η (as females would be able to obtain even more benefit via NGC by attracting high GC mates) and smaller ϵ_f (as the increasingly guaranteed 'prize' of winning the female–female competition would be higher in both GC and NGC).

Testing hypotheses against data. As outlined in the material and methods section, we were able to test two of our model's predictions against empirical data. First, our model predicts that species with larger group sizes will have more visual ovulation signs present. Figure 4*a* shows these breakdowns: species with 'present' and 'absent' visual ovulation signs have different distributions of group size. As predicted by our model, species with 'absent' visual ovulation signs are more likely to have smaller group sizes, while species with 'present' visual ovulation signs are more likely to have larger group sizes. The mean group size for species with 'absent' visual ovulation signs is 18.67, while the mean group size for species with 'present' visual ovulation signs is 37.41, a 100% increase. After testing for significance using a simulation-based phylogenetic ANOVA test [60,61], we found these differences to be significant ($F = 12.868$, $p = 0.002$).

Second, our model predicted that species with a higher risk of infanticide (i.e. higher average L/G) would have more visual ovulation signs present. Figure 4*b* depicts the box plots of L/G for species with 'absent' and 'present' ovulation signs visible. We see that, as predicted, the mean L/G value for species with 'absent' ovulation signs is less than the mean for species with 'present' ovulation signs, and in general they have different distributions, in line with our model's prediction. After considering phylogeny using [63], there is still support for this correlation between infanticide risk (L/G) and visual ovulation signs (62% relative probability from model selection; see the electronic supplementary material for more details).

4. Discussion

Here, we have developed a framework for modelling the evolution of visual female sexual signalling, allowing for both

possible benefits of paternity concentration and paternity confusion. In general, we have shown that increased visual ovulation signalling could have evolved for a variety of reasons. For example, our model predicts increased visual ovulation signals with increased group size (N), increased variation in male quality (b), decreased costs of having ovulation signs visible (c), increased effects of infanticide (α, β, κ), increased weight of male genetic quality (i.e. decreased η), increased male reproductive inequality (i.e. decreased ϵ_m), and increased correlation between male-provided genetic and non-genetic benefits (ρ). These predictions are all testable.

Overall, we see a costs trade-off between ovulation signs magnitude (m) and ovulation signs length (ℓ). In situations where strong ovulation signs magnitude is favoured (for example, when males evaluate their paternity exclusively on the basis of female signs; $\kappa = 1$), we typically see smaller ℓ^*. Intuitively, a female will only have so much energy/resources to spend on visual ovulation signalling. When strong ovulation signs magnitude is favoured, the female will invest that energy allotment on such magnitude rather than the length of her visual ovulation signal. Hence, where we see a much larger m^*, we typically see a smaller ℓ^*.

Our results show the evolution of ovulation signalling can be driven by indirect genetic benefits. A major conclusion of our work is that females can evolve sexual signalling even in the absence of genetic benefits provided by males (i.e. when $\eta = 1$). As expected [64], the effects of 'good genes' can, however, be trumped by direct costs. Moreover, the effects of good genes in our model are much weaker than those of infanticide.

It is important to note that we never intended to formalize and then test specific verbal arguments (such as the reliable indicator hypothesis against the graded signal hypothesis, which, as we discussed above, have overlapping elements and some vagueness). Rather, our approach was to start with major evolutionary forces (including different types of selection) known to act in natural populations and then investigate the effects of various parameters—group size, infanticide, genetic versus non-genetic male benefits, etc.

Our theoretical work is helpful in clearing up past confusion. Contrary to some expectations (see the Introduction), both our modelling and empirical work support greater infanticide risk leading to increased ovulation signs rather than concealed ovulation. Another example is provided by Charles Nunn's statement regarding paternity confusion, '[It] is not able to explain the conspicuousness of [the visual ovulation] signal. This hypothesis also cannot explain why features of exaggerated swellings bias certainty towards certain males in the social group.' [12, p. 238]. However, our modelling results show that the 'conspicuousness of this signal' does not have to be a result of the selection pressures owing to infanticide, but rather to one or more of the potential ecological costs identified here. Moreover, our model shows that the risk of infanticide can indeed explain why exaggerated swellings would bias certainty towards 'certain males' (i.e. more powerful/effective ones). Such males are both more likely to take over a group from a current alpha-male (and hence the risk of infanticide from them be imminent), and more likely to be stronger/better able to protect a female's infant from any possible infanticide attempt by a new alpha-male.

Our work complements the sparse earlier modelling work on visual ovulation signalling. Pagel [25] used mathematical modelling to argue that male–male competition for females will always occur and to support the reliable indicator hypothesis. Huchard *et al.* [52] used agent-based simulations, attempting to reconcile the reliable indicator and graded signal hypotheses. They showed the reliable indicator hypothesis by itself to be viable and also concluded that mate choice for a direct benefit like fertility could lead to an indirect benefit like good genes. Nakahashi [53] modelled the coevolution of ovulation signs and male mating behaviour, assuming that males can estimate the fertility of females with whom they mate; he did not model the effects of infanticide explicitly. Compared to these earlier efforts, our model explores a much wider range of evolutionary factors (including the effects of infanticide and genetic and non-genetic benefits to females) under more biologically realistic assumptions (e.g. by explicitly splitting the female cycle into discrete units of time and by assuming that males can only *estimate* the fertility of females with whom they mate, rather than know it exactly).

Although our models aim to describe any primate species with multi-male multi-female groups, in particular there has been much interest on the question of why do *human* females have concealed ovulation [21,22]? Is this related to some larger 'adaptive suite' in human evolution [38]? While our results do not support the infanticide hypothesis for the evolution of concealed ovulation in humans [29], our model does make predictions about evolutionary dynamics which lead to several new hypotheses for why concealed ovulation may have evolved in our ancestors.

In particular, such ecological causes for the disappearance of visual ovulation signals could include: (i) group size decreasing (potentially as a result of changes in ecological resource distributions, predators, etc.), (ii) within-group variation in male quality decreasing or males becoming more egalitarian [65,66], (iii) non-genetic components of male quality becoming highly beneficial compared to genetic components, (iv) physiological costs of having ovulation signs increasing (owing to increased water retention, body weight, infection/damage, predation, etc.; potentially as a result of the adaptation of bipedalism), and/or (v) the effects of infanticide decreasing. Note with regard to (i) above, visual ovulation signs are expected to disappear with the transition to monogamy since the benefits of visual ovulation signalling (i.e. attracting good and/or more mates) disappear, while the costs remain present [38,67]. This is in line with both previous phylogenetic studies on the primate mating system and visual ovulation signs [49,50], and also our model should we set $N = 1$.

Our approach comes with several limitations. Like many models, we assume discrete generations for mathematical simplicity. We also assume an additive fitness function. Explicitly accounting for the female cycle has made obtaining informative analytical results not feasible, leading to us rely on agent-based simulations. In our model, we did not impose female cycle synchrony. Assuming so would increase female–female competition and hence ovulation signalling. We do not consider the effects of any extended mate-guarding (i.e. mate-guarding lasting longer than our one discrete unit of time). We do not explicitly allow for variation in signal reliability, instead assuming a female's peak day of fertility and day of peak visible ovulation signs to line up. We also only consider multi-male, multi-female mating systems, excluding other mating systems from direct consideration in our model. In addition, our description of 'male quality' is purposefully general; we do not explicitly take into account male age, rank or any other similar known factor in primate mating.

While much work still needs to go into understanding the evolution of visual female sexual signalling, our model is able to resolve some old controversies and shed new light on this important issue. In particular, our work suggests several ecological pathways by which visual ovulation signals could have evolved or diminished, while also showing that infanticide can provide important selection pressure on the evolution of visual ovulation signs. Aside from the two predictions explored in figure 4, applying more of our theoretical insights to other specific systems/species would require further detailed information on fitness components and ecological factors, which we hope to have inspired for future empirical work.

Data accessibility. All supporting data are available in our online electronic supplementary material.

Author's contributions. K.R. and S.G. designed research, analysed data and wrote the paper.

Competing interests. We declare we have no competing interests.

Funding. K.R. was supported by a NSF Graduate Research Fellowship. S.G. was supported by the National Institute for Mathematical and Biological Synthesis through the NSF awards EF-0832858 and DBI-1300426, with additional support from The University of Tennessee. All numerical simulations were run on the Volos cluster, which is supported by the NIH award GM56693 (S.G.).

Acknowledgments. We thank J. Beaulieu for the help with the phylogenetic analysis, and J. Auerbach for the comments and suggestions. We also thank the editor and reviewers for their useful comments.

Appendix A. Model details

Females. The female fertility function is assumed to have a triangular shape with zero probability of fertilization outside of a female's C fertile days (see the electronic supplementary material, figure S1). Given female traits $m_i \geq 0$ (ovulation signs magnitude) and $\ell_i \in \mathbb{Z}$, $\ell_i \in [0, D]$ (ovulation signs length), the amount $x_i(d)$ of ovulation signs visible on any day d of the cycle is defined as

$$x_i(d) = \begin{cases} m_i \cdot \left[1 - \left(\frac{2|d - \lceil \ell_i/2 \rceil|}{\ell_i + 1}\right)^{\gamma}\right] & \text{for } d = 1, 2, \ldots, \ell_i \\ 0 & \text{otherwise} \end{cases} \quad \text{(A 1)}$$

for $\gamma > 0$ (note figure 2 depicts $x_i(d)$ with $\gamma = 2$) and d measured from the start of ovulation signs being visible. Note m_i represents the peak of $x_i(d)$ and ℓ_i the width of the non-zero portion of $x_i(d)$. Traits m and ℓ are treated as controlled by two unlinked haploid loci. Mutation effects in m_i are randomly chosen from a normal distribution $N(0, \sigma^2)$, whereas mutations in ℓ_i are discrete, representing adding or subtracting exactly one day to or from a female's time of having ovulation signs visible.

Males. Male-provided genetic (y_g) and non-genetic (y_{ng}) benefits are randomly drawn from the bivariate normal distribution, each with mean $\hat{y}$ and standard deviation b, and correlation parameter ρ; parameter $\hat{y}$ characterizes mean male quality and $b > 0$ the extent of variation. Males are ranked according to the value of their genetic quality: $y_{g,j}$ such that $y_{g,1} > y_{g,2} > \ldots$ for each male j. Small b implies small additional benefits to females from investing in ovulation signalling. For simplicity, the distribution of male quality in the population remains constant, e.g. as a result of mutation-selection balance.

Mating pairs. On each day, mating pairs are formed by first randomly perturbing both the male trait y_g and female trait x by adding to each an independent, normally distributed random variable with standard deviation $\epsilon_m \geq 0$ and $\epsilon_f \geq 0$, respectively. Males and females are then sorted according to these perturbed values and mating occurs between individuals of the same order.

Female fertility. In the case of no infanticide, we define female fitness (fertility) as

$$w_i = w_0 + (1 - \eta) y_{g,i} + \eta \tilde{y}_{ng} - c \cdot \bar{x}_i. \quad \text{(A 2)}$$

Here, w_0 is the baseline fitness, $y_{g,i}$ the genetic benefit provided by the male who fertilizes female i, $\tilde{y}_{ng} = (1/D) \sum_{(\text{all mates } j)} y_{ng,j}$ the average non-genetic benefit provided by all female i's mates, and $c \cdot \bar{x}_i$ the costs to a female of supporting her visual ovulation signs with $\bar{x}_i = (1/D) \sum_{d=1}^{D} x_i(d)$, a female's average visual ovulation signs. Our choice of the cost term implies that there is a fitness trade-off between the m and ℓ traits so that having large values of both traits implies very large fitness costs.

Infanticide. Each male in a female's group can affect her fitness directly, because of infanticide, although males will differ in the effectiveness of their actions' (e.g. owing to strength, rank, size and alliances). We assume each male's effectiveness to be proportional to $f(j)$ for each male j (sorted by males' y_g) via an exponential function: $f(j) \sim e^{-\omega j}$ with parameter $\omega > 0$ controlling the amount of disparity among males in their corresponding effectiveness within the group. Note a larger value of ω indicates more disparity, and $\omega = 0$ equality.

A male's contribution $g(p_j)$ to female fitness (positive via helping protect the offspring, or negative via not helping and/or harming the offspring) depends on his perceived probability of paternity p_j. Adapted from van Schaik *et al.* [24], we define $g(p_j) = \alpha[1 - \beta(1 - p_j)^{\tau}]$, with parameters α, $\beta > 0$ and $\tau \geq 1$. Note α determines the maximum benefit a female can obtain from a male protecting her offspring from infanticide, while $\alpha(1 - \beta)$ determines the maximum cost a female can incur from a male *not* protecting her offspring from infanticide. The overall effect of infanticide on female fitness (that gets added to the right-hand side of equation 2) is $\sum_j f(j) g(p_j)$, summing over all males j. Note whenever $\alpha = 0$, there are no effects of infanticide.

A male, in general, would not know his actual paternity probability and would instead have to estimate it, when deciding on protecting an infant or committing infanticide. Consider male j mating with female i with visible ovulation signs $x_i(d)$. We postulate that the male-estimated ('perceived') probability p_j of being the father of her offspring is proportional to $(x_i(d))^{\kappa}$ where $\kappa \in [0, 1]$ is the weight males put on visual ovulation signs. With multiple matings with the same female, we sum up the corresponding terms $(x_i(d))^{\kappa}$.

Simulations. This model was implemented independently in both C++ and MATLAB with similar results. Migration occurs with only females migrating between groups, although simulations were also run with only males migrating between groups and the results were unaffected. Mutation occurs with a mutation rate per gene per generation of 10^{-3}. $2N$ offspring are created in each group every generation, with N female and N male, determined randomly. The expected number of offspring per female is 2; the actual number is random, proportional to each female's fitness.

The agent-based model uses 16 different initial conditions in all simulations: every combination of $m = 0, 0.3, 0.6, 0.9$ and $\ell = 1, 2, 3, 4$. Parameters used include: $G = 400$; $T = 100,000$; $D = 29$; $C = 7$ (with probabilities of fertilization on

each of these days being 0.125, 0.25, 0.375, 0.5, 0.375, 0.25, 0.125, respectively); $w_0 = 1$; $N = 4, 8, 16$; $b = 0.1, 0.2, 0.4$; $c = 0.1, 0.2, 0.4$; $\eta = 0.25, 0.5, 0.75$; $\rho = -0.5, 0, 0.5$; $\gamma = 0.5, 1, 2$; $\hat{y} = 1$; $\sigma = \sqrt{0.1}$; $\epsilon_m = 0, 0.25, 0.5$; $\epsilon_f = 0, 0.01, 0.05$, $\alpha = 0, 0.2, 0.6, 1$; $\beta = 1.25, 1.5, 1.75$; $\tau = 1, 2, 4$; $\omega = 0, 1, 2$; and $\kappa = 0, 0.5, 1$. Further information on parameter values tested and each of their effects is available in the electronic supplementary material.

References

1. Darwin C. 1871 *The descent of man and selection in relation to sex*. London, UK: J. Murray.
2. Andersson MB. 1994 *Sexual selection*. Princeton, NJ: Princeton University Press.
3. Hosken DJ, House CM. 2011 Sexual selection. *Curr. Biol.* **21**, R62–R65.
4. Andersson M, Iwasa Y. 1996 Sexual selection. *Trends Ecol. Evol.* **11**, 53–58. (doi:10.1016/0169-5347(96)81042-1)
5. Kokko H, Brooks R, Jennions MD, Morley J. 2003 The evolution of mate choice and mating biases. *Proc. R. Soc. Lond. B* **270**, 653–664. (doi:10.1098/rspb.2002.2235)
6. Clutton-Brock T. 2016 *Mammal societies*. Oxford, UK: Wiley.
7. Pusey A, Schroepfer-Walker K. 2013 Female competition in chimpanzees. *Phil. Trans. R. Soc. B* **368**, 20130077. (doi:10.1098/rstb.2013.0077)
8. Clutton-Brock T. 2009 Sexual selection in females. *Anim. Behav.* **77**, 3–11. (doi:10.1016/j.anbehav.2008.08.026)
9. Servedio MR, Lande R. 2006 Population genetic models of male and mutual mate choice. *Evolution* **60**, 674–685. (doi:10.1111/j.0014-3820.2006.tb01147.x)
10. Darwin C. 1876 Sexual selection in relation to monkeys. *Nature* **15**, 18–19. (doi:10.1038/015018a0)
11. Zinner DP, van Schaik CP, Nunn CL, Kappeler PM. 2004 Sexual selection and exaggerated sexual swellings of female primates. In *Sexual selection in primates: new and comparative perspectives* (eds PM Kappeler, CP van Schaik), ch. 5, pp. 71–89. Cambridge, UK: Cambridge University Press.
12. Nunn CL. 1999 The evolution of exaggerated sexual swellings in primates and the graded-signal hypothesis. *Anim. Behav.* **58**, 229–246. (doi:10.1006/anbe.1999.1159)
13. Dixson AF. 2012 *Primate sexuality*, 2nd edn. New York, NY: Oxford University Press.
14. Dixson AF. 1983 Observations on the evolution and behavioral significance of 'sexual skin' in female primates. In *Advances in the study of behavior* (eds JS Rosenblatt, RA Hinde, MC Busnell), vol. 13, pp. 63–106. London, UK: Academic Press, Inc.
15. Hrdy SB, Whitten PL. 1987 Patterning of sexual activity. In *Primate societies* (eds BB Smuts, DL Cheney, RM Seyfarth, RW Wrangham, TT Struhsaker), ch. 5, pp. 370–384. Chicago, IL: University of Chicago Press.
16. Krohn PL, Zuckerman S. 1937 Water metabolism in relation to the menstrual cycle. *J. Physiol. (Lond.)* **88**, 369–387. (doi:10.1113/jphysiol.1937.sp003447)
17. Clutton-Brock TH, Harvey PH. 1976 Evolutionary rules and primate societies. In *Growing points in ethology* (eds PPG Bateson, RA Hinde), ch. 6, pp. 195–237. Cambridge, UK: Cambridge University Press.
18. Williams JM, Oehlert GW, Carlis JV, Pusey AE. 2004 Why do male chimpanzees defend a group range? *Anim. Behav.* **68**, 523–532. (doi:10.1016/j.anbehav.2003.09.015)
19. Scarry CJ, Tujague MP. 2012 Consequences of lethal intragroup aggression and alpha male replacement on intergroup relations and home range use in tufted capuchin monkeys (*Cebus apella nigritus*). *Am. J. Primatol.* **74**, 804–810. (doi:10.1002/ajp.22030)
20. Lovejoy CO. 1981 The origin of man. *Science* **211**, 341–350. (doi:10.1126/science.211.4480.341)
21. Gangestad SW, Thornhill R. 2008 Human oestrus. *Proc. R. Soc. B* **275**, 991–1000. (doi:10.1098/rspb.2007.1425)
22. Thornhill R, Gangestad SW. 2008 *The evolutionary biology of human female sexuality*. New York, NY: Oxford University Press.
23. Dixson AF. 2009 *Sexual selection and the origins of human mating systems*, 1st edn. New York, NY: Oxford University Press.
24. van Schaik CP, Pradhan GR, van Noordwijk MA. 2004 Mating conflict in primates: infanticide, sexual harassment and female sexuality. In *Sexual selection in primates* (eds PM Kappeler, CP van Schaik), ch. 8, pp. 131–150. Cambridge, UK: Cambridge University Press.
25. Pagel M. 1994 The evolution of conspicuous oestrous advertisement in Old World monkeys. *Anim. Behav.* **47**, 1333–1341. (doi:10.1006/anbe.1994.1181)
26. Burt A. 1992 'Concealed ovulation' and sexual signals in primates. *Folia Primatologica* **58**, 1–6. (doi:10.1159/000156600)
27. Hamilton III WJ. 1984 Significance of paternal investment by primates to the evolution of adult male-female associations. In *Primate paternalism* (ed. DM Taub), pp. 309–335. New York, NY: van Nostrand Reinhold.
28. Alberts SC, Fitzpatrick CL. 2012 Paternal care and the evolution of exaggerated sexual swellings in primates. *Behav. Ecol.* **23**, 699–706. (doi:10.1093/beheco/ars052)
29. Hrdy S. 1981 *The woman that never evolved*. Cambridge, MA: Harvard University Press.
30. Dixson A. 2002 Sexual selection by cryptic female choice and the evolution of primate sexuality. *Evol. Anthropol.* **11**, 195–199. (doi:10.1002/evan.10090)
31. Stallman RR, Froehlich JW. 2000 Primate sexual swellings as coevolved signal systems. *Primates* **41**, 1–16. (doi:10.1007/BF02557457)
32. Hrdy S. 1979 Infanticide among animals. *Ethol. Sociobiol.* **1**, 13–40. (doi:10.1016/0162-3095(79)90004-9)
33. Van Noordwijk MA, van Schaik CP. 2000 Reproductive patterns in eutherian mammals: adaptations against infanticide? In *Infanticide by males and its implications* (eds CP van Schaik, CH Janson), ch. 14, pp. 322–360. New York, NY: Cambridge University Press.
34. Paul A. 2002 Sexual selection and mate choice. *Int. J. Primatol.* **23**, 877–904.
35. Zipple MN, Grady HJ, Gordon JB, Chow LD, Archie EA, Altmann J, Alberts SC. 2017 Conditional fetal and infant killing by male baboons. *Proc. R. Soc. B* **284**, 20162561. (doi:10.1098/rspb.2016.2561)
36. Pradhan GR, van Schaik CP. 2008 Infanticide-driven intersexual conflict over matings in primates and its effects on social organization. *Behavior* **145**, 251–275. (doi:10.1163/156853907783244710)
37. van Schaik CP. 2000 Social counterstrategies against male infanticide in primates and other mammals. In *Primate males: causes and consequences of variation in group composition* (ed. PM Kappeler), ch. 4, pp. 34–52. New York, NY: Cambridge University Press.
38. Lovejoy CO. 2009 Reexamining human origins in light of *Ardipithecus ramidus*. *Science* **326**, 74–74e8. (doi:10.1126/science.1175834)
39. Palombit RA. 1999 Infanticide and the evolution of pair bonds in nonhuman primates. *Evol. Anthropol.* **7**, 117–129. (doi:10.1002/(SICI)1520-6505(1999)7:43.0.CO;2-0)
40. Nunn CL, van Schaik CP, Zinner D. 2001 Do exaggerated sexual swellings function in female mating competition in primates? a comparative test of the reliable indicator hypothesis. *Behav. Ecol.* **12**, 646–654. (doi:10.1093/beheco/12.5.646)
41. Domb LG, Pagel M. 2001 Sexual swellings advertise female quality in wild baboons. *Nature* **410**, 204–206. (doi:10.1038/35065597)
42. Zinner D, Alberts SC, Nunn CL, Altmann J. 2002 Significance of primate sexual swellings. *Nature* **420**, 142–143. (doi:10.1038/420142a)
43. Deschner T, Heistermann M, Hodges K, Boesch C. 2004 Female sexual swelling size, timing of ovulation, and male behavior in wild West African chimpanzees. *Horm. Behav.* **46**, 204–215. (doi:10.1016/j.yhbeh.2004.03.013)
44. Setchell JM, Wickings EJ. 2004 Sexual swelling in mandrills (*Mandrillus sphinx*): a test of the reliable indicator hypothesis. *Behav. Ecol.* **15**, 438–445. (doi:10.1093/beheco/arh027)
45. Higham JP, Heistermann M, Saggau C, Agil M, Perwitasari-Farajallah D, Engelhardt A. 2012

Sexual signalling in female crested macaques and the evolution of primate fertility signals. *BMC. Evol. Biol.* **12**, 1–10. (doi:10.1186/1471-2148-12-89)

46. Fitzpatrick CL, Altmann J, Alberts SC. 2014 Sources of variance in a female fertility signal: exaggerated estrous swellings in a natural population of baboons. *Behav. Ecol. Sociobiol.* (*Print*) **68**, 1109–1122. (doi:10.1007/s00265-014-1722-y)
47. Fitzpatrick CL, Altmann J, Alberts SC. 2015 Exaggerated sexual swellings and male mate choice in primates: testing the reliable indicator hypothesis in the amboseli baboons. *Anim. Behav.* **104**, 175–185. (doi:10.1016/j.anbehav.2015.03.019)
48. Douglas PH, Hohmann G, Murtagh R, Thiessen-Bock R, Deschner T. 2016 Mixed messages: wild female bonobos show high variability in the timing of ovulation in relation to sexual swelling patterns. *BMC Evol. Biol.* **16**, 1–17.
49. Sillen-Tullberg B, Moller AP. 1993 The relationship between concealed ovulation and mating systems in anthropoid primates: a phylogenetic analysis. *Am. Nat.* **141**, 1–25. (doi:10.1086/285458)
50. Pagel M, Meade A. 2006 Bayesian analysis of correlated evolution of discrete characters by reversible-jump Markov chain Monte Carlo. *Am. Nat.* **167**, 808–825. (doi:10.1086/503444)
51. Gouzoules H, Gouzoules S. 2002 Primate communication: by nature honest, or by experience wise? *Int. J. Primatol.* **23**, 821–848. (doi:10.1023/A:1015529032135)
52. Huchard E, Courtiol A, Benavides JA, Knapp LA, Raymond M, Cowlishaw G. 2009 Can fertility signals lead to quality signals? insights from the evolution of primate sexual swellings. *Proc. R. Soc. B* **276**, 1889–1897. (doi:10.1098/rspb.2008.1923)
53. Nakahashi W. 2016 Coevolution of female ovulatory signals and male-male competition in primates. *J. Theor. Biol.* **392**, 12–22. (doi:10.1016/j.jtbi.2015.12.007)
54. van Schaik CP, van Noordwijk MA, Nunn CL. 1999 Sex and social evolution in primates. In *Comparative primate socioecology* (ed. PC Lee), ch. 8, pp. 204–240. New York, NY: Cambridge University Press.
55. Jones KE *et al.* 2009 Pantheria: a species-level database of life history, ecology, and geography of extant and recently extinct mammals. *Ecology* **90**, 2648. (doi:10.1890/08-1494.1)
56. Kamilar JM, Cooper N. 2013 Phylogenetic signal in primate behaviour, ecology and life history. *Phil. Trans. R. Soc. B* **368**, 20120341. (doi:10.1098/rstb.2012.0341)
57. Atmoko SSU, van Schaik CP. 2010 The natural history of sumatran orangutan (*Pongo abelii*). In *Indonesian primates* (eds S Gursky-Doyen, J Supriatna), ch. 4, pp. 41–56. New York, NY: Springer.
58. Binford LR. 2001 *Constructing frames of reference*. Berkeley, MA: University of California Press.
59. Opie C, Atkinson QD, Dunbar RIM, Shultz S. 2013 Male infanticide leads to social monogamy in primates. *Proc. Natl Acad. Sci. USA* **110**, 13 328–13 332. (doi:10.1073/pnas.1307903110)
60. Garland Jr T, Dickerman AW, Janis CM, Jones JA. 1993 Phylogenetic analysis of covariance by computer simulation. *Syst. Biol.* **42**, 265–292. (doi:10.1093/sysbio/42.3.265)
61. Revell LJ. 2012 Phytools: an R package for phylogenetic comparative biology (and other things). *Methods Ecol. Evol.* **3**, 217–223. (doi:10.1111/j.2041-210X.2011.00169.x)
62. Fabre PH, Rodrigues A, Douzery EJP. 2009 Patterns of macroevolution among primates inferred from a supermatrix of mitochondrial and nuclear DNA. *Mol. Phylogenet. Evol.* **53**, 808–825. (doi:10.1016/j.ympev.2009.08.004)
63. Beaulieu JM, Jhwueng D-C, Boettiger C, O'Meara BC. 2012 Modeling stabilizing selection: expanding the Ornstein-Uhlenbeck model of adaptive evolution. *Evolution* **66**, 2369–2383. (doi:10.1111/j.1558-5646.2012.01619.x)
64. Kirkpatrick M. 1985 Evolution of female choice and male parental investment in polygynous species: the demise of the 'sexy son'. *Am. Nat.* **125**, 788–810. (doi:10.1086/284380)
65. Boehm C. 2001 *Hierarchy in the forest: the evolution of egalitarian behavior*. Cambridge, MA: Harvard University Press.
66. Gavrilets S. 2012 On the evolutionary origins of the egalitarian syndrome. *Proc. Natl Acad. Sci. USA* **109**, 14 069–14 074. (doi:10.1073/pnas.1201718109)
67. Gavrilets S. 2012 Human origins and the transition from promiscuity to pair-bonding. *Proc. Natl Acad. Sci. USA* **109**, 9923–9928. (doi:10.1073/pnas.1200717109)

Supplementary Information for:

On the evolution of visual female sexual signalling

Kelly Rooker and Sergey Gavrilets

Contents

Further Details of the Model

The Female Cycle

Female estrous cycles are divided into D discrete units of time (e.g. $D = 29$ days) with $C \leq D$ days of fertility (e.g. $C = 7$). Although the form of such fertile periods will be identical in all females, the timing of each fertile period will be randomly distributed among females. For instance, when $C = 7$ (calling each of these fertile days $C1$, $C2$, ... , $C7$) and $D = 29$ (calling each of these days $D1$, $D2$, ... , $D29$), $C1$ in every female has an equal probability of landing on any of $D1$, $D2$, ... , $D29$. Since C is a cycle, we similarly assume $C7$ can land on any such day. For example, if $C1$ landed on $D24$, then $C7$ would 'wrap around' the cycle to land on $D1$. Moreover, for all females we assume ovulation happens directly in the middle of this C cycle. Hence, for $C = 7$ we assume ovulation happens on $C4$ and the probabilities of fertilization increase from $C1$ to $C4$ and then decrease from $C4$ to $C7$.

Since having visible ovulation signs at least loosely correlates with a female's fertility, we assume the day(s) of having maximum visual ovulation signs align with the day(s) of that female's maximum fertilization probability, and align these cycles accordingly (note in many cases, $C \neq \ell_i$). Recall $x_i(d)$ denotes the amount of visual ovulation signs present on each day d of the female cycle, with $x_i(d)$ defined by the function

$$x_i(d) = \begin{cases} m_i \cdot \left[1 - \left(\frac{2|d - \lceil \ell_i/2 \rceil|}{\ell_i + 1}\right)^{\gamma}\right] & \text{for } d = 1, 2, ..., \ell_i \\ 0 & \text{otherwise} \end{cases} \tag{S1}$$

This function is determined by m_i (ovulation signs magnitude), ℓ_i (ovulation signs length), and parameter γ (controlling the shape of the resulting curve). Note the exact function $x_i(d)$ is chosen such that (i) m_i will denote the peak of the curve, (ii) ℓ_i will denote the width of the non-zero portion of the curve, (iii) m_i, ℓ_i remain independent of each other, and (iv) m_i, ℓ_i can each decrease all the way to zero. Example values of $x_i(d)$ are displayed in Fig. S1 for varying values of m_i, ℓ_i, and γ, with $C = 7$ (as indicated by the red shaded bars).

Determining Male-Female Mate Pairs

We assume that, for every day of the cycle, males of higher GC will preferentially mate with females with more ovulation signs visible. We also assume each individual to mate precisely once on each day of the cycle. Parameters ε_m and ε_f control the amount of stochasticity in the process of mating pair formation. On each day, mating pairs are formed by first randomly perturbing both the male trait y_g and female trait x by adding to each an independent, normally distributed random variable with standard deviation $\varepsilon_m \geq 0$ and $\varepsilon_f \geq 0$, respectively (i.e. $x' = x + e_x, y'_g = y_g + e_y$, where $e_x \sim N(0, \varepsilon_f^2), e_j \sim N(0, \varepsilon_m^2)$). Males and females are then sorted according to these perturbed values and mating occurs between individuals of the same order. With $\varepsilon_m, \varepsilon_f \to \infty$, mating pairs are formed completely independently of the values of x_i and $y_{g,j}$.

Calculating Probabilities of Paternity

To calculate the probability of paternity for each male, first the fertility of each female with which that male mated is summed up for every day a particular male mates with that female. These values are normalized across males for each female in the group, meaning a male who mates with a female on day(s) where she has a higher fertility probability will have a higher paternity probability. The actual father for that female's offspring is then determined randomly, proportional to each male's probability of paternity for her offspring.

Note these *actual* probabilities of paternity are different from the *perceived* probabilities of paternity, as detailed in the main text. We make this distinction because a male will not know any female's probability of fertility at the time he mates with her; a male will only know how many visible ovulation signs she has present. Separating these quantities allows *actual* probabilities of paternity (which males do not know) to be calculated using females' probabilities of fertility, and *perceived* probabilities of paternity (which males *do* know) to be calculated using females' visible ovulation signs.

Infanticide

We define the exponential function of male effectiveness to be

$$f(j) = \frac{e^{-\omega j}}{\sum_{k=1}^{N} e^{-\omega k}}, \tag{S2}$$

with parameter $\omega > 0$ controlling the amount of disparity among males in their corresponding effectiveness within a group. Recall a larger value of ω indicates more disparity among males.

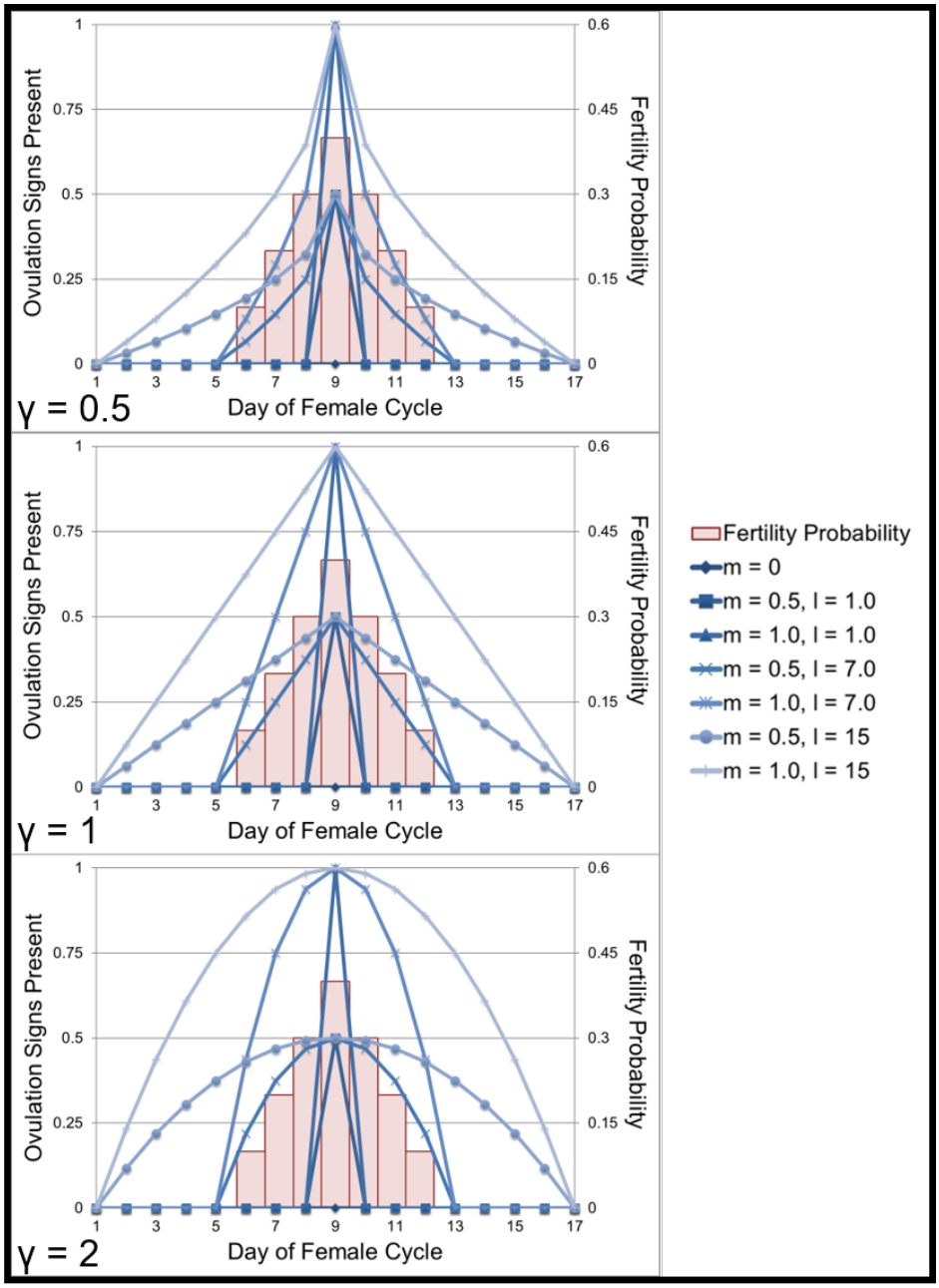

Figure S1: For each day d of a female cycle, sample values for visual ovulation signs present, $x_i(d)$, are displayed for $\gamma = 0.5, 1, 2$ (from top to bottom). Each graph includes all combinations of $\ell_i = 1, 7, 15$ and $m_i = 0, 0.5, 1$. Note $C = 7$ in this example, with fertility probabilities depicted by the red shaded bars. $x_i(d) = 0$ on a red shaded day means the female has no signs present on day d, despite still having some positive probability of fertilization. Conversely, positive $x_i(d)$ values *outside* the shaded days indicate visual ovulation signs being present despite a zero probability of fertilization.

We define the function for male contributions to offspring survival to be

$$g(p) = \alpha[1-\beta(1-p)^{\tau}], \tag{S3}$$

with parameters $\alpha, \beta > 0$ and $\tau \geq 1$. α determines the maximum benefit a female can obtain from a male protecting her offspring from infanticide, while $\alpha(1-\beta)$ determines the maximum cost a female can incur from a male *not* protecting her offspring from infanticide. Note whenever $\alpha = 0$, there are no effects of infanticide on infant survival.

Female Fitness Functions

The fitness function for female i in the model is

$$w_i = w_0 + (1-\eta)y_{g,i} + \eta\tilde{y}_{ng} + \sum_{j=1}^{N}\left[f(j)g(p_{i,j})\right] - c\bar{x}_i, \tag{S4}$$

Here, w_0 is baseline fitness, $y_{g,i}$ the genetic benefit provided by the male who fertilizes female i, $\tilde{y}_{ng} = \frac{1}{D}\sum_{(\text{all mates } j)} y_{ng,j}$ the average non-genetic benefit provided by all female i's mates, $p_{i,j}$ the perceived paternity probability of male j for female i's offspring, and $c \cdot \bar{x}_i$ the costs to a female of supporting her visual ovulation signs with $\bar{x}_i = \frac{1}{D}\sum_{d=1}^{D} x_i(d)$, a female's average visual ovulation signs.

Recall that fitness is each female's relative reproductive success (the expected number of offspring surviving to the age of reproduction), normalized to keep the total population size in each generation constant. As such, this fitness measure incorporates various fitness components, including female and offspring viability and female fertility. The division of fitness into separate benefits and costs terms follows the tradition in evolutionary game theory. The baseline constant w_0 is the fitness of a female with no ovulation signs present, mating with the worst genetic-quality male in the case of no infanticide and no non-genetic benefits. The absolute values of the other terms are relative to w_0 and specify the strength of selection. Rather than separately modelling various fitness components, we follow the standard approach in evolutionary modelling by wrapping them into female fitness via the benefits and costs terms.

Notice for the case when $\alpha = 0$ and, thus, $g = 0$ (i.e. without the effects of infanticide), the fitness function above collapses into

$$w_i = w_0 + (1-\eta)y_{g,i} + \eta\tilde{y}_{ng} - c\bar{x}_i, \tag{S5}$$

Note in this $\alpha = 0$ (no infanticide) case, parameters β, κ, τ, and ω all become unnecessary.

Evolutionary Dynamics

Numerical simulations of our model show that the average values of the ovulation signs magnitude trait (m) and the ovulation signs length trait (ℓ) converge to the unique equilibria m^*, ℓ^*. Fig. S2 illustrates the evolution of m (x-axis) and ℓ (y-axis) over time, both with and without the effects of infanticide included. In particular, we see that introducing infanticide increases m^*.

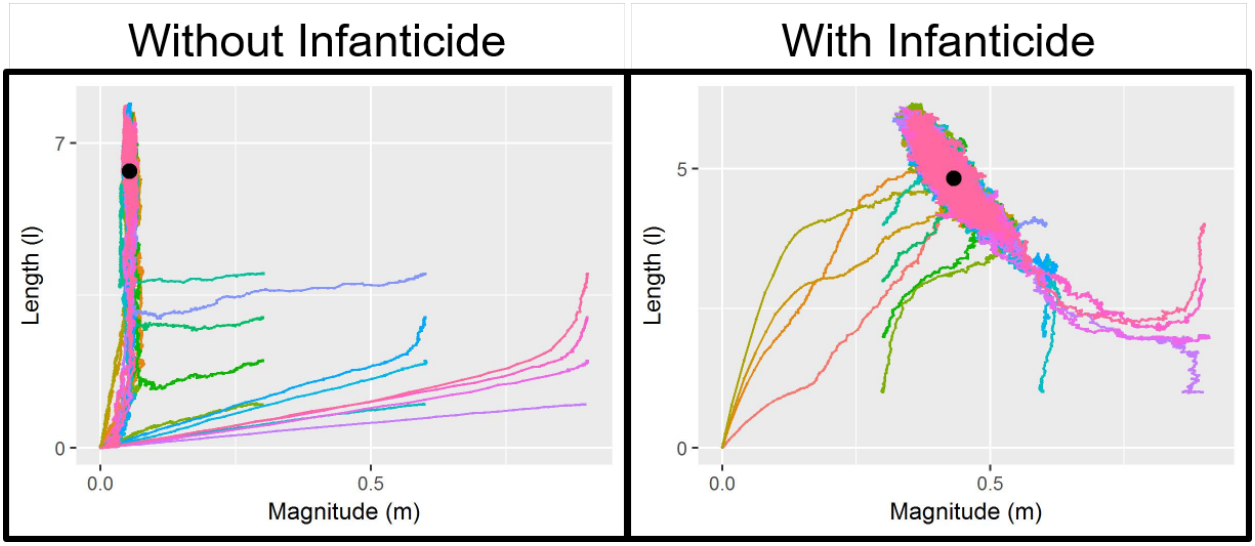

Figure S2: Example evolutionary dynamics on the phase plane (m, ℓ), both without (left graph) and with (right graph) infanticide. Each graph depicts simulations of the model for 16 different initial conditions (illustrated by the different-coloured lines). Notice introducing infanticide increases magnitude m^*, and we see convergence in all cases, as illustrated by the black points depicting the averages over all runs at the end of the simulations. ($\alpha = 0$ (left) and $\alpha = 1$ (right) with all other parameters held constant: $N = 16$, $b = 0.2$, $c = 0.2$, $\varepsilon_m = 0.25$, $\varepsilon_f = 0.01$, $\omega = 1$, $\tau = 2$, $\beta = 1.75$, $\kappa = 1$, $\gamma = 1$, $\eta = 0.5$, $\rho = 0$.)

List of All Parameters

Parameters used in the model are as follows (with one value listed below implying the parameter remained fixed throughout all simulations, and multiple values indicating each of those parameter values was tested in all combinations with all other parameters):

$G = 400$	Number of groups
$T = 100000$	Time (number of generations)
$D = 29$	Number of days in each female's cycle
$C = 7$	Number of days each female has non-zero probability of fertilization
$C_v = \{0.125, 0.25, 0.375, 0.5, 0.375, 0.25, 0.125\}$	Probability of fertilization on each of those C = 7 days
$w_0 = 1$	Baseline female fitness
$N = 4, 8, 16$	Number of males and number of females in each group
$b = 0.1, 0.2, 0.4$	Variation in male quality
$c = 0.1, 0.2, 0.4$	Weighting of the cost of having ovulation signs present
$\eta = 0.25, 0.5, 0.75$	Weighting of NGC vs. GC on female fitness
$\rho = -0.5, 0, 0.5$	Correlation between a male's GC and NGC
$\hat{y} = 1$	Mean male quality
$\varepsilon_m = 0, 0.25, 0.5$	Parameter determining the amount of reproductive stochasticity among males
$\varepsilon_f = 0, 0.01, 0.05$	Parameter determining the amount of reproductive stochasticity among females
$\gamma = 0.5, 1, 2$	Parameter determining the shape of the function for the amount of visual ovulation signs present
$\alpha = 0, 0.2, 0.6, 1$	Parameter controlling the maximum benefit of protecting against infanticide (note α = 0 corresponds to the case with NO infanticide)
$\beta = 1.25, 1.5, 1.75$	Parameter controlling the relative maximum cost of infanticide in the paternity probability effect function
$\tau = 1, 2, 4$	Exponent in the paternity probability effect function
$\omega = 0, 1, 2$	Parameter in the male effectiveness function $f(j)$
$\kappa = 0, 0.5, 1$	Parameter determining the weight males put on the amount of visual ovulation signs in their paternity estimates
$\nu = 1$	Migration rate (between zero and one)
$\mu = 0.001$	Probability of mutation (per gene per generation)
$\sigma = \sqrt{0.1}$	Standard deviation for mutation magnitude

Table S1: List of All Parameters

Effects of All Parameters

Found in Figure:	Increasing Parameter:	Results Primarily In:	Rationale:
3(a), S3	N	*increasing* the ovulation traits	Increased competition for high-GC mates
	b	*increasing* the ovulation traits	Increased variation in male quality
	c	*decreasing* the ovulation traits	Increased costs of having signs
3(b), S4, S6	α	*increasing* the ovulation traits	Increased effects of infanticide
	β	*increasing* the ovulation traits	Increased effects of infanticide
3(b), S4	κ	*increasing* the ovulation signs magnitude trait and *decreasing* the ovulation signs length trait	Increased competition for high-GC mates increases m, while the higher m goes, the lower ℓ goes, due to fitness cost trade-offs
3(c), S3, S4, S5	η	*decreasing* the ovulation traits	Increased weighting on NGC vs. GC
3(c), S5	ε_m	*decreasing* the ovulation traits	Decreased likelihood of obtaining a high-quality male even when winning female-female competition
	ε_f	*increasing* the ovulation signs magnitude trait and *decreasing* the ovulation signs length trait	Effects dependent on ε_m, but in general the more reproductive stochasticity among females, the more females concentrate their signal stronger and on fewer days
3(d), S3, S4, S5, S6	ρ	*increasing* the ovulation traits	Increased benefit to females from mating with high-GC males
S5	γ	*decreasing* the ovulation traits	Increased visual ovulation signs for any given values of m and ℓ
S6	τ	*increasing* the ovulation traits	Increased effects of infanticide
	ω	*increasing* the ovulation signs magnitude trait and *decreasing* the ovulation signs length trait	Increased competition for high-GC mates increases m, while the higher m goes, the lower ℓ goes, due to fitness cost trade-offs

Table S2: Effects of All Parameters

Note the intuition behind the effects of N, b, c, α, β, κ, η, ρ, ε_m, and ε_f are discussed in the main text. Increasing γ results in decreasing the ovulation signs traits. This is expected since γ changes the shape of the ovulation signs curve (see Fig. S1). With a larger γ, for any fixed m_i, ℓ_i, and d, $x_i(d)$ will be larger. Thus with a larger γ, to get the same $x_i(d)$ for all d, one would now need *smaller* m_i, ℓ_i.

Increasing τ increases the benefit a female obtains from protection against infanticide, and hence (as discussed in the main text) also the ovulation signs traits.

Finally, increasing ω results in increasing ovulation signs magnitude (m) and decreasing ovulation signs length (ℓ) because increasing ω results in a larger disparity among males in terms of their effectiveness within a group. As this disparity, and hence competition for high-GC males, increases, it becomes in females' best interests to allocate more energy/resources towards ovulation signs magnitude vs. ovulation signs length. This difference is because having more ovulation signs present than any other female in the group, even if just present on one day, will make it more likely for that female to secure a copulation with a high-GC male.

ANOVA Results

We ran an analysis of variance (ANOVA) to determine which of ovulation signs magnitude m and ovulation signs length ℓ are affected most by which parameters. In general, we find that the results summarized in Table S2 reflect those of these ANOVAs.

The following tables (Tables S3, S4, S5, S6) give the detailed results of these tests. Each table below reflects the results from different simulation sets. The numbers in each of these tables correspond to percentage of variance, with the sign ($\pm$) corresponding to the direction of the effect. Any table entry with a zero means that effect is not significant (i.e. $p > 0.05$). For example, in Table S3, 41% of the variation in ovulation signs magnitude (m) in this simulation set can be explained by parameter b, and another 17% by parameter c. Since the effect of b is positive and c negative, we know that as b increases, m also increases, and as c increases, m instead decreases. Each of the following tables can be interpreted in this fashion.

Table S3: Percentage of variance of N, b, c, η, ρ on ovulation signs magnitude M and length L

	M	L
N	0.03	0.01
b	0.41	0.53
c	-0.17	-0.08
η	-0.11	-0.08
ρ	0.01	0.04
error	0.27	0.27

Table S4: Percentage of variance of $\alpha, \beta, \kappa, \eta, \rho$ on ovulation signs magnitude M and length L

	M	L
α	0.39	0.17
β	0.02	0
κ	0.38	-0.35
η	-0.01	0.02
ρ	0	0.05
error	0.20	0.41

Table S5: Percentage of variance of $\varepsilon_m, \varepsilon_f, \gamma, \eta, \rho$ on ovulation signs magnitude M and length L

	M	L
ε_m	-0.36	-0.05
ε_f	0	-0.48
γ	-0.02	-0.01
η	-0.39	-0.02
ρ	0.01	0.06
error	0.28	0.38

Table S6: Percentage of variance of $\alpha, \beta, \omega, \tau, \rho$ on ovulation signs magnitude M and length L

	M	L
α	0.32	0.04
β	0.02	0
ω	0.28	-0.57
τ	0.11	0.02
ρ	0	0
error	0.28	0.37

Extra Figures

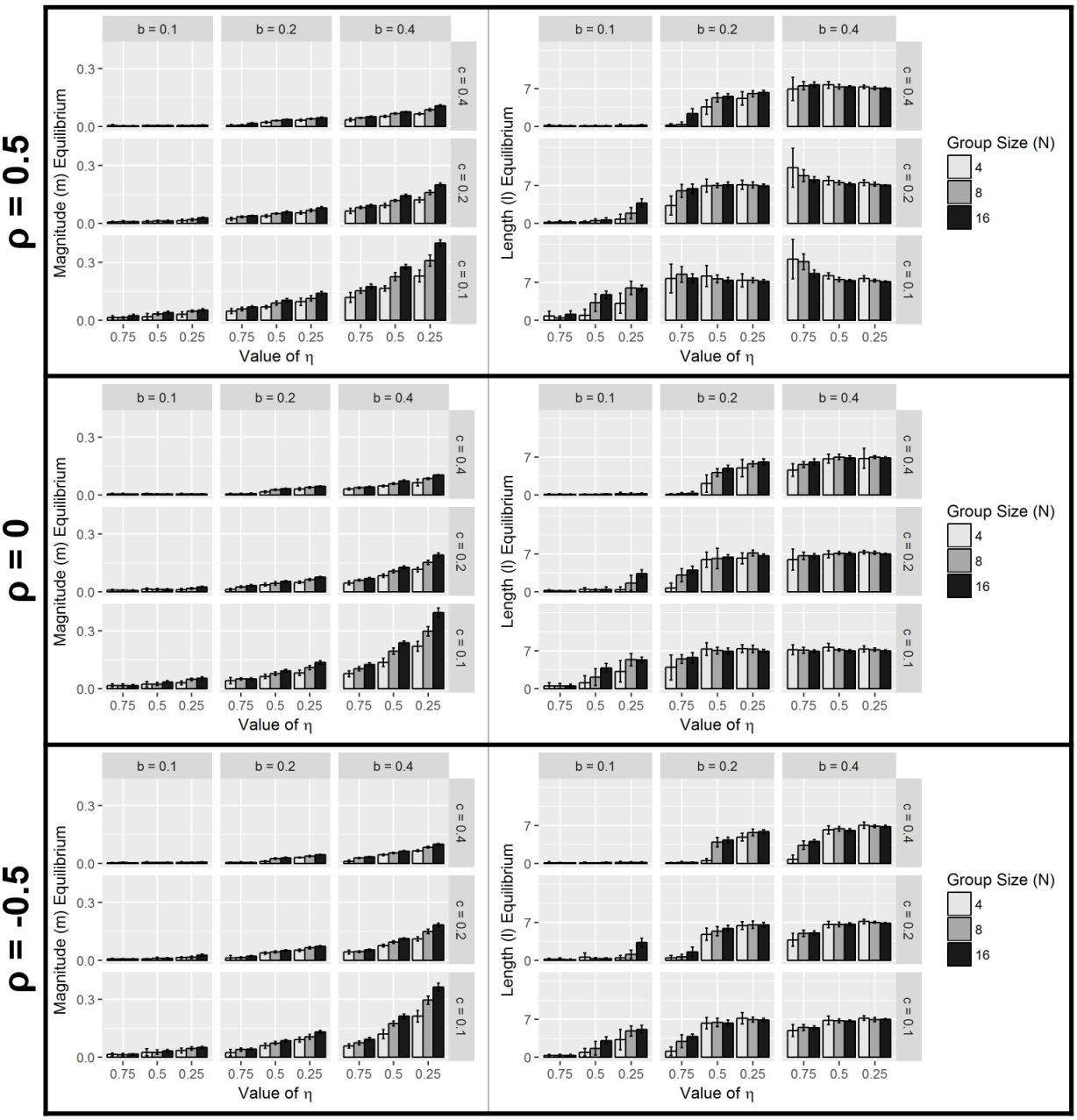

Figure S3: The effects of parameters N (group size), b (variation in male quality), c (costs of having ovulation signs), and η (relative weighting of NGC) on the average equilibria values of magnitude m (left graphs) and length ℓ (right graphs) for three different values of ρ (from top to bottom). Equilibria are obtained by averaging over 16 initial condition runs (with standard deviation indicated by error bars). All other parameters were held constant: $\varepsilon_m = 0.25, \varepsilon_f = 0.01, \gamma = 1, \alpha = 0$.

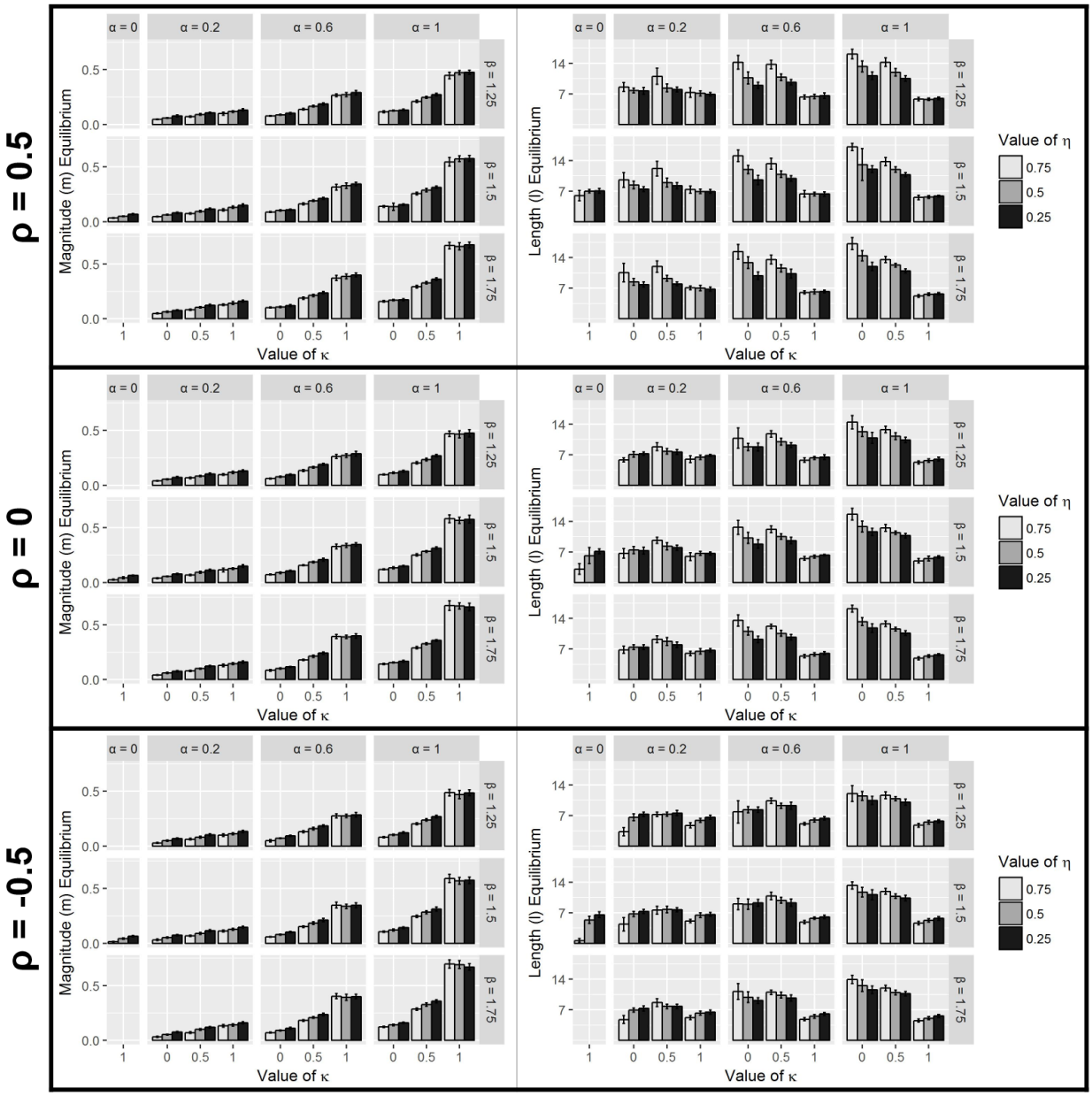

Figure S4: The effects of parameters α (maximum benefit of infanticide), β (proportional to the maximum cost of infanticide), κ (weight males put on females having ovulation signs visible), and η (relative weighting of NGC) on the average equilibria values of both magnitude m (left graphs) and length ℓ (right graphs) for three different values of ρ (from top to bottom). Equilibria are obtained by averaging over 16 initial condition runs (with standard deviation indicated by error bars). All other parameters were held constant: $N = 8, b = 0.2, c = 0.2, \varepsilon_m = 0.25, \varepsilon_f = 0.01, \gamma = 1$.

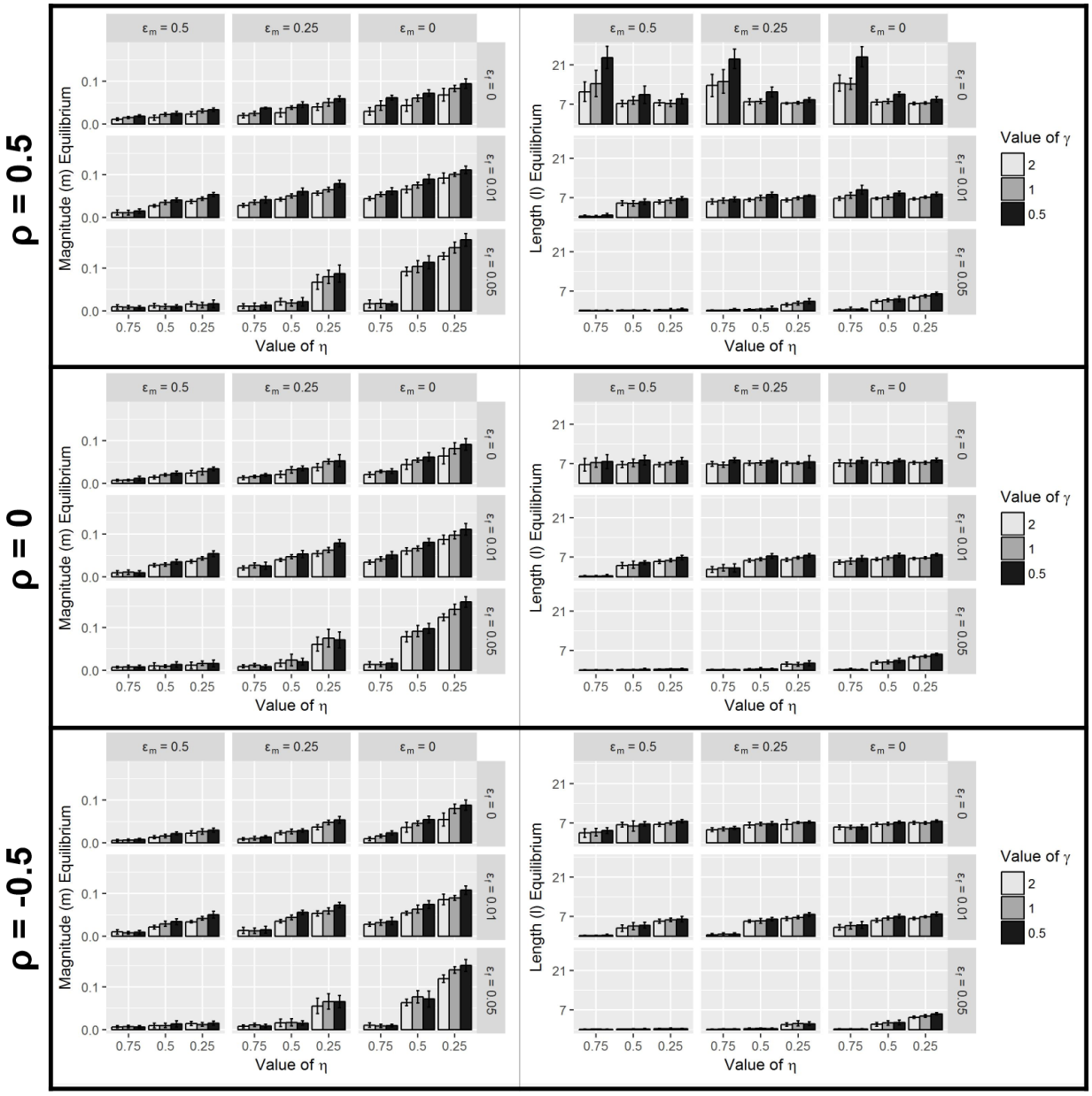

Figure S5: The effects of parameters ε_m (reproductive stochasticity among males), ε_f (reproductive stochasticity among females), γ (determines shape of x_i curve), and η (relative weighting of NGC) on the average equilibria values of both magnitude m (left graphs) and length ℓ (right graphs) for three different values of ρ (from top to bottom). Equilibria are obtained by averaging over 16 initial condition runs (with standard deviation indicated by error bars). All other parameters were held constant: $N = 8, b = 0.2, c = 0.2, \alpha = 0$.

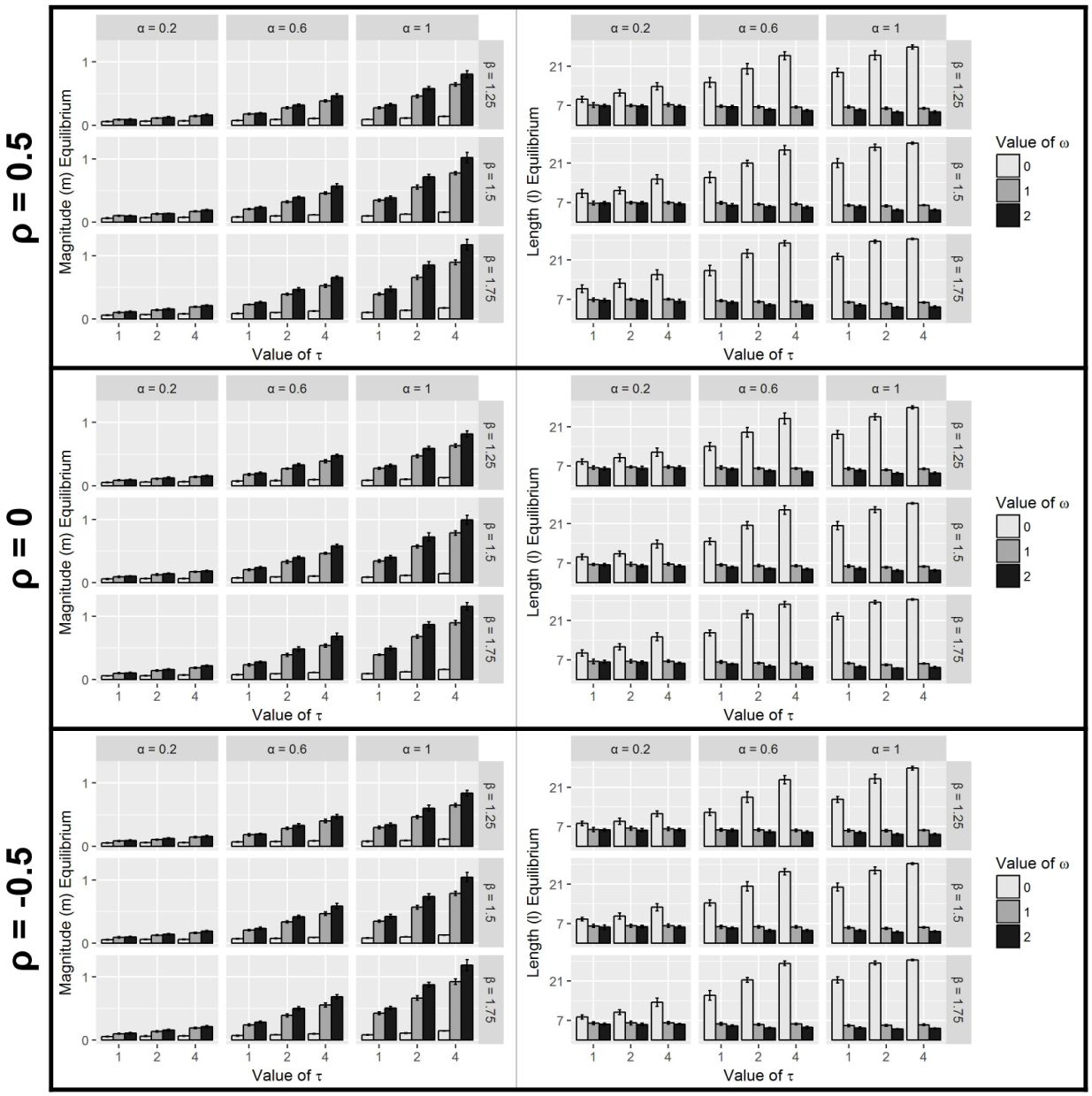

Figure S6: The effects of parameters α (maximum benefit of infanticide), β (proportional to the maximum cost of infanticide), τ (non-linearities in g), and ω (determines shape of $f(j)$) on the average equilibria values of both magnitude m (left graphs) and length ℓ (right graphs) for three different values of ρ (from top to bottom). Equilibria are obtained by averaging over 16 initial condition runs (with standard deviation indicated by error bars). All other parameters were held constant: $N = 8, b = 0.2, c = 0.2, \varepsilon_m = 0.25, \varepsilon_f = 0.01, \gamma = 1, \kappa = 1, \eta = 0.5$.

Empirical Data

Statistical Tests

Two empirical comparisons were outlined in the main text between: (1) visible ovulation signs and group size, and (2) visible ovulation signs and risk of infanticide. Information for the phyloANOVA test for (1) is presented comprehensively in the main text.

We can also test both (1) and (2) using more powerful likelihood-based methods. An overview, as applied to infanticide risk, is included in the main text. Model comparison for this test uses 5 different models: bm1 (single-rate Brownian motion), bms.root (Brownian motion with different rate parameters for each state on a tree, taken from the root), bms.means (Brownian motion with different rate parameters for each state on a tree, taken from the means), ou1 (Ornstein-Uhlenbeck model with a single optimum for all species), and oum (Ornstein-Uhlenbeck model with different state means). In particular, we compare Ornstein-Uhlenbeck models with one vs. multiple optima for the trait of interest. In the case of only one single optimum, the trait is assumed to evolve non-neutrally but that all species (regardless of Present vs. Absent visible ovulation signs) are pulled towards that one single optimal value. With multiple optima (one for species with Present visible ovulation signs and the other for species with Absent visible ovulation signs), species with Present vs. Absent visible ovulation signs have different average values of the trait. See Beaulieu (2012) for further details on each of these five models and their implementations.

For example, comparing models ou1 and oum in our test of group size, model ou1 being favoured implies there is no difference in group size means between species with "Absent" and "Present" ovulation signs, while model oum being favoured implies there *is* a difference in the two group size means for species with "Absent" and "Present" ovulation signs. The values in the following table give the normalized AICw (relative likelihoods) for each of these five models for each of our two tests.

	bm1	**bms.root**	**bms.means**	**ou1**	**oum**
Group Size	0.043	0.17	0.17	0.17	0.45
Infanticide Risk	$<$0.001	$<$0.001	$<$0.001	0.38	0.62

Table S7: Results of Statistical Tests

With a frequentist type of test like phyloANOVA, the p-value will be strongly impacted by sample size, while with AIC, it deals with information. This means if the information is strong in the data, sample size will not matter with respect to fitting the data well (but will have an impact on the uncertainty in the parameter estimates). The group size test is able to include more primate species than the infanticide test, simply because there is more data for average group size compared to infanticide risk (potentially because group size is an easier trait to measure empirically). The infanticide test has a stronger overall AICw for the oum model than the group size test does, despite the group size phyloANOVA reaching significance while the infanticide test did not. We believe this effect to be due to the sample size available to use for each test.

Raw Data

Starting on the following page is a table depicting the empirical data used in constructing Fig. 5 of the main text. The first two columns give the Family and Species Names, respectively. The third

column depicts the species' mating system, as classified by Opie et.al. (2013). The fourth column ("Visible Ovulation Signs") gives the amount of ovulation signs visible ("Absent", "Slight", or "Present"). The fifth column ("Group Size") gives the average group size for each species. The sixth, seventh, and eighth columns ("Lactation Length", "Gestation Length", "Lactation / Gestation") give the average length of lactation, average length of gestation, and ratio of "Lactation Length" to "Gestation Length", respectively. Sources for all data in columns 4-7 are listed in the main text. Any cell left empty signifies missing data from these sources for that particular species/trait.

Table S8: Complete Raw Primate Data

Family Name	Species Name	Mating System	Ovulation Signs	Group Size	Weaning Age (L)	Gestation Length (G)	L/G
Cercopithecini	Allenopithecus_nigroviridis	Polygynandrous	Present	40			
Lemuriformes	Allocebus_trichotis	Monogamous		1			
Atelidae	Alouatta_caraya	Polygynous/Polygynandrous	Absent	8	325	187	1.74
Atelidae	Alouatta_palliata	Polygynous/Polygynandrous	Slight	12	325	186	1.75
Atelidae	Alouatta_pigra	Polygynous/Polygynandrous		6.6			
Atelidae	Alouatta_sara	Polygynous/Polygynandrous			371	191	1.94
Atelidae	Alouatta_seniculus	Polygynous/Polygynandrous	Slight	7.1	372	191	1.95
Cebidae	Aotus_azarae	Monogamous	Absent	3.1			
Cebidae	Aotus_lemurinus_griseimembra	Monogamous	Absent		75	133	0.56
Cebidae	Aotus_nancymaae	Monogamous	Absent	3.9	75	131	0.57
Cebidae	Aotus_trivirgatus	Monogamous	Absent	2.9	75	133	0.56
Loridae	Arctocebus_aureus	Polygynous			115	134	0.86
Loridae	Arctocebus_calabarensis	Polygynous		1	105	135	0.78
Atelidae	Ateles_belzebuth	Polygynandrous	Absent	22.125			
Atelidae	Ateles_fusciceps	Polygynandrous	Absent		486	226	2.15
Atelidae	Ateles_geoffroyi	Polygynandrous	Absent	15	750	225	3.33
Atelidae	Ateles_geoffroyi_panamensis	Polygynandrous	Absent				
Atelidae	Ateles_geoffroyi_vellerosus	Polygynandrous	Absent				
Atelidae	Ateles_geoffroyi_yucatanensis	Polygynandrous	Absent				
Atelidae	Ateles_paniscus	Polygynandrous	Absent	18.2	760	230	3.30
Lemuriformes	Avahi_laniger	Monogamous		3	150	136.15	1.10
Lemuriformes	Avahi_occidentalis	Monogamous		3.5			
Atelidae	Brachyteles_arachnoides	Polygynandrous	Absent	20.9	638	233	2.74
Hominoidea	Bunopithecus_hoolock	Monogamous	Absent/Slight				
Pitheciidae	Callicebus_donacophilus	Monogamous	Absent	1			
Pitheciidae	Callicebus_moloch	Monogamous	Absent	3.3	60	164	0.37
Cebidae	Callimico_goeldii	Polygynous/Monogamous	Absent	7.2	65	151	0.43
Cebidae	Callithrix_argentata	Polygynous/Monogamous	Absent	9.5			
Cebidae	Callithrix_aurita	Polygynous/Monogamous	Absent	7.5			
Cebidae	Callithrix_emiliae	Polygynous/Monogamous	Absent				
Cebidae	Callithrix_geoffroyi	Polyandrous/Monogamous	Absent	5			
Cebidae	Callithrix_humeralifera	Polygynous/Monogamous	Absent	8.5			

Cebidae	Callithrix_jacchus	Polyandrous/Monogamous	Absent	11	60	148	0.41
Cebidae	Callithrix_kuhlii	Polygynous/Monogamous	Absent	5			
Cebidae	Callithrix_penicillata	Polygynous/Monogamous	Absent	8			
Cebidae	Callithrix_pygmaea	Monogamous	Absent	2	90	137	0.66
Cebidae	Cebus_albifrons	Polygynandrous	Absent	25.1	269	155	1.74
Cebidae	Cebus_apella	Polygynandrous	Absent	12.9	261	154	1.69
Cebidae	Cebus_capucinus	Polygynandrous	Absent	16.4	510	162	3.15
Papionini	Cercocebus_agilis	Polygynandrous	Present	21.5			
Papionini	Cercocebus_galeritus	Polygynandrous	Present	18.2			
Papionini	Cercocebus_torquatus	Polygynandrous	Present	26.9			
Papionini	Cercocebus_torquatus_atys	Polygynandrous	Present	90			
Cercopithecini	Cercopithecus_ascanius	Polygynous	Absent	28.8	146	172	0.85
Cercopithecini	Cercopithecus_campbelli_lowei	Polygynous		14	362	180	2.01
Cercopithecini	Cercopithecus_cephus	Polygynous	Absent	8	362	170	2.13
Cercopithecini	Cercopithecus_diana	Polygynous	Absent	24			
Cercopithecini	Cercopithecus_hamlyni	Polygynous	Absent				
Cercopithecini	Cercopithecus_lhoesti	Polygynous	Absent	17.4			
Cercopithecini	Cercopithecus_mitis	Polygynous	Absent	18.6	692	140	4.94
Cercopithecini	Cercopithecus_mona	Polygynous	Absent	4.8			
Cercopithecini	Cercopithecus_neglectus	Polygynous/Monogamous	Absent	4.5	365	165	2.21
Cercopithecini	Cercopithecus_nictitans	Polygynous	Slight	13			
Cercopithecini	Cercopithecus_petaurista	Polygynous		11.3			
Cercopithecini	Cercopithecus_preussi	Polygynous		3			
Cercopithecini	Cercopithecus_solatus	Polygynous		10			
Lemuriformes	Cheirogaleus_crossleyi	Monogamous			45	70	0.64
Lemuriformes	Cheirogaleus_major	Monogamous	Slight	1	70	71	0.99
Lemuriformes	Cheirogaleus_medius	Polygynous/Monogamous	Slight	1	61	62	0.98
Cercopithecini	Chlorocebus_aethiops	Polygynandrous	Absent	19.5			
Cercopithecini	Chlorocebus_pygerythrus	Polygynandrous	Slight		201	163	1.23
Colobinae	Colobus_angolensis	Polygynandrous	Absent/Slight	18.25			
Colobinae	Colobus_guereza	Polygynous	Absent	12	330	170	1.94
Colobinae	Colobus_polykomos	Polygynandrous	Absent/Slight	11	215	170	1.26
Lemuriformes	Daubentonia_madagascariensis	Polygynandrous	Slight	1	170	164	1.04
Cercopithecini	Erythrocebus_patas	Polygynous	Slight	28.2	213	167	1.28

Lemuriformes	Eulemur_coronatus	Polygynandrous		9.25			
Lemuriformes	Eulemur_fulvus_albifrons	Polygynandrous			135	120	1.13
Lemuriformes	Eulemur_fulvus_albocollaris	Polygynandrous			135	120	1.13
Lemuriformes	Eulemur_fulvus_collaris	Polygynandrous		7	135	120	1.13
Lemuriformes	Eulemur_fulvus_fulvus	Polygynandrous		8.9	135	120	1.13
Lemuriformes	Eulemur_fulvus_mayottensis	Polygynandrous			135	120	1.13
Lemuriformes	Eulemur_fulvus_rufus	Polygynandrous		9.17	135	120	1.13
Lemuriformes	Eulemur_fulvus_sanfordi	Polygynandrous		5	135	120	1.13
Lemuriformes	Eulemur_macaco	Polygynandrous	Slight	10	135	129	1.05
Lemuriformes	Eulemur_mongoz	Monogamous		2.93	152	129	1.18
Lemuriformes	Eulemur_rubriventer	Monogamous		3			
Galagonidae	Euoticus_elegantulus	Polygynandrous		1			
Galagonidae	Galago_alleni	Polygynous		6			
Galagonidae	Galago_moholi	Polygynandrous		1	84	123	0.68
Galagonidae	Galago_senegalensis	Polygynandrous	Slight	1	98	142	0.69
Galagonidae	Galagoides_demidoff	Polygynous/Monogamous		10	45	110	0.41
Galagonidae	Galagoides_zanzibaricus	Polygynous/Monogamous		1	59	126	0.47
Hominoidea	Gorilla_beringei	Polygynous	Slight	11.1			
Hominoidea	Gorilla_gorilla	Polygynous	Slight	7.1	1278	260	4.92
Lemuriformes	Hapalemur_aureus	Monogamous		3	140	138	1.01
Lemuriformes	Hapalemur_griseus_griseus	Polygynous/Monogamous		4.4	120	140	0.86
Lemuriformes	Hapalemur_simus	Polygynandrous		7.5			
Hominoidea	Homo_sapiens	Polygynous/Monogamous	Absent	17.49	730	267	2.73
Hominoidea	Hylobates_agilis	Monogamous	Slight	4.2			
Hominoidea	Hylobates_klossii	Monogamous	Slight	3	330	210	1.57
Hominoidea	Hylobates_lar	Monogamous	Slight	3.3	548	205	2.67
Hominoidea	Hylobates_moloch	Monogamous	Slight	2.15			
Hominoidea	Hylobates_muelleri	Monogamous	Slight	3.2			
Hominoidea	Hylobates_pileatus	Monogamous	Slight	3.25			
Lemuriformes	Indri_indri	Monogamous		3.2	363	159	2.28
Atelidae	Lagothrix_lagotricha	Polygynandrous	Absent	33.1	315	223	1.41
Lemuriformes	Lemur_catta	Polygynandrous	Slight	17	120	141	0.85
Cebidae	Leontopithecus_chrysomelas	Polygynous/Monogamous	Absent	6.7			
Cebidae	Leontopithecus_chrysopygus	Monogamous	Absent	3.6			

Cebidae	Leontopithecus_rosalia	Polygynous/Monogamous	Absent	5.4	90	129	0.70
Lemuriformes	Lepilemur_dorsalis	Polygynous		1			
Lemuriformes	Lepilemur_edwardsi	Monogamous		2			
Lemuriformes	Lepilemur_leucopus	Polygynous		1	121.66	130	0.94
Lemuriformes	Lepilemur_microdon	Polygynous		1			
Lemuriformes	Lepilemur_mustelinus	Polygynous		1	75	135	0.56
Lemuriformes	Lepilemur_ruficaudatus	Monogamous		1	119	150	0.79
Lemuriformes	Lepilemur_sahamalazensis	DD		1			
Lemuriformes	Lepilemur_septentrionalis	Polygynous			120.97	134	0.90
Papionini	Lophocebus_albigena	Polygynous/Polygynandrous	Present	15.8	210	186	1.13
Papionini	Lophocebus_aterrimus	Polygynous/Polygynandrous	Present	17.5			
Loridae	Loris_lydekkerianus_malabaricus	Polygynandrous			135	167	0.81
Loridae	Loris_tardigradus	Polygynandrous/Monogamous	Slight	2	170	166	1.02
Papionini	Macaca_arctoides	Polygynandrous	Absent	31.1	393	178	2.21
Papionini	Macaca_assamensis	Polygynandrous	Slight	21			
Papionini	Macaca_brunnescens	Polygynandrous	Present				
Papionini	Macaca_cyclopis	Polygynandrous	Present	20.2	206	162	1.27
Papionini	Macaca_fascicularis	Polygynandrous	Present	27.5	330	160	2.06
Papionini	Macaca_fuscata	Polygynandrous	Slight	53.7	365	173	2.11
Papionini	Macaca_hecki	Polygynandrous	Present				
Papionini	Macaca_maura	Polygynandrous	Present				
Papionini	Macaca_mulatta	Polygynandrous	Slight	40.7	192	165	1.16
Papionini	Macaca_nemestrina	Polygynandrous	Present	18.2	234	167	1.40
Papionini	Macaca_nigra	Polygynandrous	Present	63.8			
Papionini	Macaca_nigrescens	Polygynandrous	Present	14.5			
Papionini	Macaca_ochreata	Polygynandrous	Present				
Papionini	Macaca_radiata	Polygynandrous	Absent	30	365	162	2.25
Papionini	Macaca_silenus	Polygynandrous	Present	19.6	365	180	2.03
Papionini	Macaca_sinica	Polygynandrous	Absent	24.5			
Papionini	Macaca_sylvanus	Polygynandrous	Present	18.2	210	165	1.27
Papionini	Macaca_thibetana	Polygynandrous	Slight	38.3	561	170	3.30
Papionini	Macaca_tonkeana	Polygynandrous	Present				
Papionini	Mandrillus_leucophaeus	Polygynandrous	Present	17			
Papionini	Mandrillus_sphinx	Polygynandrous	Present	13.9	348	175	1.99

Lemuriformes	Microcebus_murinus	Polygynandrous	Slight	1	40	60	0.67
Lemuriformes	Microcebus_myoxinus	Polygynandrous		1			
Lemuriformes	Microcebus_rufus	Polygynandrous		1	40	57	0.70
Cercopithecini	Miopithecus_talapoin	Polygynandrous	Present	66.5	180	162	1.11
Lemuriformes	Mirza_coquereli	Polygynandrous	Slight	1	136	87	1.56
Colobinae	Nasalis_larvatus	Polygynous	Slight	12	210	166	1.27
Hominoidea	Nomascus_concolor	Monogamous	Absent/Slight	4			
Hominoidea	Nomascus_gabriellae	Monogamous	Absent/Slight	1			
Hominoidea	Nomascus_leucogenys	Monogamous	Absent/Slight	1			
Loridae	Nycticebus_coucang	Polygynous	Slight	1	135	170	0.79
Loridae	Nycticebus_pygmaeus	Polygynous		1			
Galagonidae	Otolemur_crassicaudatus	Polygynandrous	Slight	6	135	135	1.00
Galagonidae	Otolemur_garnettii	Polygynandrous		1	140	132	1.06
Hominoidea	Pan_paniscus	Polygynandrous	Present	85.1	1080	240	4.50
Hominoidea	Pan_troglodytes	Polygynandrous	Present	63.1	1680	235	7.15
Hominoidea	Pan_troglodytes_schweinfurthii	Polygynandrous	Present		1680	235	7.15
Hominoidea	Pan_troglodytes_verus	Polygynandrous	Present		1680	235	7.15
Papionini	Papio_anubis	Polygynandrous	Present	57.7	584	180	3.24
Papionini	Papio_cynocephalus	Polygynandrous	Present	55	365	173	2.11
Papionini	Papio_hamadryas	Polygynous/Polygynandrous	Present	66.1	561	170	3.30
Papionini	Papio_papio	Polygynandrous	Present	50			
Papionini	Papio_ursinus	Polygynandrous	Present	34.7			
Loridae	Perodicticus_potto	Polygynous	Slight	2	150	170	0.88
Colobinae	Piliocolobus_badius	Polygynandrous	Present	49.4			
Hominoidea	Pongo_abelii	Polygynandrous	Absent	2	720	250	2.88
Hominoidea	Pongo_pygmaeus	Polygynandrous	Absent	2	720	250	2.88
Colobinae	Presbytis_melalophos	Polygynous/Polygynandrous		14.5			
Colobinae	Procolobus_verus	Polygynous/Polygynandrous	Present	6.3			
Lemuriformes	Propithecus_coquereli	Polygynandrous		5.5			
Lemuriformes	Propithecus_diadema	Polygynandrous/Monogamous		5.38	183	178	1.03
Lemuriformes	Propithecus_edwardsi	Polygynandrous		4.6	210	179	1.17
Lemuriformes	Propithecus_tattersalli	Polygynandrous		4.1	153	170	0.90
Lemuriformes	Propithecus_verreauxi	Polygynandrous	Slight	5	180	162	1.11
Colobinae	Pygathrix_nemaeus	Polygynous/Polygynandrous	Slight	9.3			

Colobinae	Rhinopithecus_avunculus	Polygynous	Absent/Slight	30			
Colobinae	Rhinopithecus_bieti	Polygynous	Absent/Slight	50			
Colobinae	Rhinopithecus_roxellana	Polygynous	Absent/Slight	65			
Cebidae	Saguinus_fuscicollis	Polgynous/Polyandrous/Monogamous	Absent	5.1	90	150	0.60
Cebidae	Saguinus_geoffroyi	Polygynous/Monogamous	Absent	6.3	55	145	0.38
Cebidae	Saguinus_imperator	Polgynous/Polyandrous/Monogamous	Absent	7			
Cebidae	Saguinus_midas	Monogamous	Absent	5.55	70	127	0.55
Cebidae	Saguinus_oedipus	Polygynandrous/Monogamous	Absent	5.8	50	168	0.30
Cebidae	Saimiri_boliviensis	Polygynandrous	Slight	60			
Cebidae	Saimiri_oerstedii	Polygynandrous	Slight	55.3			
Cebidae	Saimiri_sciureus	Polygynandrous	Absent	38	168	170	0.99
Colobinae	Semnopithecus_entellus	Polygynous/Polygynandrous	Absent	30.2	249	184	1.35
Hominoidea	Symphalangus_syndactylus	Monogamous	Absent	4	639	232	2.75
Tarsiidae	Tarsius_bancanus	Polygynous/Monogamous	Slight	1	79	178	0.44
Tarsiidae	Tarsius_syrichta	Polygynous/Monogamous	Slight	1	82	180	0.46
Papionini	Theropithecus_gelada	Polygynous	Present	10	540	170	3.18
Colobinae	Trachypithecus_auratus	Polygynous		14.5			
Colobinae	Trachypithecus_cristatus	Polygynous	Absent	32.4	365	195	1.87
Colobinae	Trachypithecus_francoisi	Polygynous	Absent/Slight	8.9			
Colobinae	Trachypithecus_johnii	Polygynous	Slight	10			
Colobinae	Trachypithecus_obscurus	Polygynous	Slight	10.2			
Colobinae	Trachypithecus_phayrei	Polygynous	Absent/Slight	12.9	305	205	1.49
Colobinae	Trachypithecus_pileatus	Polygynous	Absent/Slight	7.8			
Lemuriformes	Varecia_rubra	Polygynandrous/Monogamous		4.19	89	102	0.87
Lemuriformes	Varecia_variegata	Polygynandrous/Monogamous	Slight	2.8	89	102	0.87